
A UNIFIED FRAMEWORK FOR MULTIPLE-TRY METROPOLIS ALGORITHMS

A PREPRINT

✉ **Renny Doig**

Department of Statistics and Actuarial Science
Simon Fraser University
Burnaby, BC
rennyd@sfu.ca

✉ **Liangliang Wang**

Department of Statistics and Actuarial Science
Simon Fraser University
Burnaby, BC
liangliang_wang@sfu.ca

March 17, 2025

ABSTRACT

The multiple-try Metropolis (MTM) algorithm is a generalization of the Metropolis-Hastings algorithm in which the transition kernel uses a compound proposal consisting of multiple candidate draws. Since its seminal paper there have been several extensions to this algorithm. This paper presents a general framework that encompasses many of these extensions, as well as an independent comparison. To facilitate this, a deterministic Metropolis transition kernel is used to develop a procedure that derives valid acceptance probabilities for reversible Markov chain Monte Carlo algorithms, given only the proposal mechanism. Several configurations of MTM are explored in full factorial simulation experiment that compares the sampling performance of MTM algorithms with respect to non-Gaussian target distributions, multimodal sampling, and Monte Carlo error. We find that the form of the proposal distribution is the most important factor in determining algorithm performance, while the form of the weight function has negligible impact. A large number of candidate draws can improve the per-iteration performance, though improvements to the overall performance is limited by the additional computational burden introduced by multiple candidacy.

Keywords Markov chain Monte Carlo · acceptance probability · compound proposal

1 Introduction

Markov chain Monte Carlo (MCMC) methods are a broad class of algorithms that are popular for sampling from intractable probability distributions. These algorithms are iterative procedures that use a tractable proposal distribution to generate a collection of samples that are a realization of a Markov chain that has the target distribution as its stationary distribution. A fundamental MCMC algorithm is the Metropolis-Hastings (MH) algorithm [Hastings, 1970, Metropolis et al., 1953]. This algorithm iteratively generates a sample by constructing a Markovian transition kernel from a tractable proposal distribution and an acceptance probability that leaves the target distribution as the stationary distribution of the Markov chain. The standard MH algorithm can perform poorly when the target distribution exhibits adverse features such as local optima, plateaus, or a state-dependent covariance structure. The multiple-try Metropolis (MTM) [Liu et al., 2000] algorithm is a generalization of the MH algorithm that improves the proposal distribution by replacing the single proposal with a compound proposal comprising multiple candidate draws. Intuitively, by generating multiple candidates at each iteration, it is more likely that a good proposal will be drawn at each step and should result in an algorithm with better sampling performance than MH.

Extensions of the MTM algorithm tend to focus on one of two areas: the proposal distribution(s) from which the candidates are drawn [Casarin et al., 2013, Yang et al., 2019] or the weights used to select the proposal from these candidates [Gagnon et al., 2023, Pandolfi et al., 2010, 2014, Yang et al., 2019]. Additionally, adaptivity has been incorporated into the MTM algorithms in order to further improve the sampling efficiency [Fontaine and Béard, 2022, Yang et al., 2019]. Except for some recent work [Gagnon et al., 2023], there has been very little theoretical analysis

of MTM methods. Theory is often limited to a proof that the extension of the algorithm satisfies detailed balance conditions. To complement the existing demonstrations of the validity of MTM algorithms, we present a procedural framework for deriving theoretically acceptance probabilities for reversible MCMC algorithms. Based on a deterministic Metropolis kernel, we show how an acceptance probability can be derived for a given proposal mechanism such that the resulting acceptance probability will produce a reversible MCMC algorithm.

As is frequently the case in the academic literature, the papers that introduce each methodological extension use simulation primarily to demonstrate use-cases of the proposed extension and only include broader comparisons in a limited capacity. This is a practical limitation as large simulation studies of Bayesian sampling methods can bear a prohibitive computational burden. Nonetheless, an extensive simulation experiment systematically comparing all extensions of the MTM algorithm is absent from the existing literature. Discussion around using more statistically rigorous approaches to designing and analyzing simulation experiments has become more frequent in recent years [Chipman and Bingham, 2022, Gelman et al., 2002, Harwell et al., 2017, Skrdonal, 2000].

In this paper, we present a unified framework for the multiple-try Metropolis (MTM) algorithm, a generalization of the Metropolis-Hastings algorithm that employs a compound proposal mechanism consisting of multiple candidate draws. Since its introduction, several extensions to MTM have been proposed, and we consolidate these developments within a single, general framework. Additionally, we introduce a unifying method for deriving valid acceptance probabilities for reversible Metropolis algorithms, providing a theoretically grounded foundation that is applicable across a wide range of algorithm and settings. To evaluate how the configuration of an MTM algorithm affects the performance, we design a simulation experiment using a full factorial design, comparing the algorithm’s sampling efficiency, multimodal sampling capability, and Monte Carlo error of point estimates. Our results reveal that the form of the proposal distribution is the most significant determinant of performance, whereas the choice of weight function has negligible impact. Moreover, while increasing the number of candidate draws can enhance per-iteration performance, the overall improvement within a fixed computational budget is constrained by the additional computational cost. These findings offer valuable insights and suggest practical recommendations for researchers seeking to optimize the MTM algorithm for various applications.

The remainder of this paper is organized as follows. In Section 2, we introduce the theoretical foundation for deriving acceptance probabilities in reversible Metropolis algorithms and demonstrate the application of this procedure to MTM. Section 3 focuses on the construction of MTM algorithms, reviewing notable examples from the literature within the unified framework. A simulation study evaluating various MTM configurations using a full factorial experimental design is presented in Section 4. Finally, Section 5 concludes the paper with a discussion of MTM, including practical recommendations for implementation and promising directions for future research.

2 A theoretical framework for constructing MCMC algorithms

Reversible MCMC methods that are designed in the style of Metropolis and Hastings [Metropolis et al., 1953, Hastings, 1970] construct a Markov chain whose transition probability is composed of a proposal distribution $Q(\mathbf{y}|\mathbf{x})$ and an acceptance probability $a(\mathbf{x}, \mathbf{y})$. A typical proof that such an algorithm is valid involves showing that the reversibility, or detailed balance, condition is met: $\pi(\mathbf{x})Q(\mathbf{y}|\mathbf{x})a(\mathbf{x}, \mathbf{y}) = \pi(\mathbf{y})Q(\mathbf{x}|\mathbf{y})a(\mathbf{y}, \mathbf{x})$. This is sufficient to show that the stationary distribution of the Markov chain is π . This section presents an alternative procedure for constructing valid reversible MCMC algorithms. By using a deterministic proposal [Tierney, 1998] and a transformation of variables [Geyer and Moller, 1994, Green, 1995], we show how one can derive the form of the acceptance probability $a(\mathbf{x}, \mathbf{y})$ based on the proposal distribution. Because the acceptance probability, derived in this way, will produce a transition probability that leaves π as the stationary distribution, the procedure we present here can be used to derive acceptance probabilities for a wide range of novel and existing MCMC algorithms. This procedure is applied to MTM, demonstrating how the acceptance probability can be derived as well as presenting a unified framework for MTM algorithms.

2.1 Deterministic Metropolis algorithms

Let $\tilde{\pi}$ be a probability distribution over an arbitrary state space $\tilde{\mathcal{X}}$. In general, this state space may contain both continuous and discrete components, denoted \mathcal{X}_C and \mathcal{X}_D , respectively. A *deterministic Metropolis transition kernel* comprises the following two steps, based on a deterministic transformation as a proposal [Tierney, 1998].

1. The proposal is generated by applying the transformation g to the current state: $\tilde{\mathbf{y}} = g(\tilde{\mathbf{x}})$.
2. The chain then transitions to state $\tilde{\mathbf{y}}$ with probability

$$a(\tilde{\mathbf{x}}, \tilde{\mathbf{y}}) = 1 \wedge \frac{\tilde{\pi}(g(\tilde{\mathbf{x}}))}{\tilde{\pi}(\tilde{\mathbf{x}})} |J(g_C(\tilde{\mathbf{x}}_C))|, \quad (1)$$

where $J(g_C(\tilde{\mathbf{x}}_C))$ is the Jacobian of the continuous component of the transformation, or remains in state $\tilde{\mathbf{x}}$ with probability $1 - a(\tilde{\mathbf{x}}, \tilde{\mathbf{y}})$.

In order to ensure that the deterministic Metropolis transition kernel will produce a reversible transition probability, the following condition must be met.

Assumption 1 (Involution). The transformation g must be an involution, that is $g(g(\tilde{\mathbf{x}})) = \tilde{\mathbf{x}}$.

Theorem 1 *If Assumption 1 is satisfied and the acceptance probability is of the form given in Equation 1, then the deterministic Metropolis transition kernel will satisfy the detailed balance condition and therefore produce a reversible Markov chain that has $\tilde{\pi}$ as its stationary distribution.*

The proof of Theorem 1 is in the Supplementary Materials.

This deterministic Metropolis algorithm motivates a procedure for deriving acceptance probabilities of reversible MCMC algorithms that use a probabilistic proposal. Suppose we have an MCMC algorithm targeting π that is at current state \mathbf{x} and whose proposal generates \mathbf{y} . This procedure, which will be described presently, defines $\tilde{\pi}$ to be the joint distribution over \mathbf{x} and \mathbf{y} , as well as all intermediate or auxiliary variables that are generated. By using Equation 1 to derive an acceptance probability, one can construct valid transition kernels for MCMC methods based only on the proposal mechanism.

Assumption 2 (Marginality). The target distribution π can be recovered as a marginal distribution of $\tilde{\pi}$.

Furthermore, if Assumption 2 is met then a sample of π can be easily extracted from a sample of $\tilde{\pi}$. The following procedure outlines how we may cast a probabilistic Metropolis method as a deterministic Metropolis kernel on an extended space so that the acceptance probability can be derived according to Equation 1. This will be followed by a concrete example.

1. **Define the extended state space**, $\tilde{\mathbf{x}}$, includes all random variables generated in a single iteration of the algorithm. Then, specify the joint probability distribution over this extended space, $\tilde{\pi}(\tilde{\mathbf{x}})$.
2. **Define the involution**, $g(\tilde{\mathbf{x}})$, that defines the transformation applied to the extended state space if the proposal is accepted.
3. **Compute the Jacobian** of the continuous component of the involution: $J(g_C(\tilde{\mathbf{x}}))$.
4. **Verify that the target distribution**, $\pi(\mathbf{x})$, is a marginal distribution of the extended joint distribution, $\tilde{\pi}(\tilde{\mathbf{x}})$.
5. **Derive the acceptance probability** using Equation 1.

As a simple demonstration, consider the Metropolis-Hastings (MH) algorithm. The algorithm is targeting π as its stationary distribution. Let the current state of the chain be \mathbf{x} , and \mathbf{y} be generated from the proposal distribution $T(\cdot|\mathbf{x})$. In the MH algorithm, the only two random variables are the current state and the proposed state, so the extended state space can be defined as $\tilde{\mathbf{x}} = [\mathbf{x}, \mathbf{y}]$. The joint probability distribution over this extended space is then given by $\tilde{\pi}(\tilde{\mathbf{x}}) = \pi(\mathbf{x})T(\mathbf{y}|\mathbf{x})$. Since the first coordinate of $\tilde{\mathbf{x}}$ is the state of the Markov chain, the acceptance of \mathbf{y} as the next state in the chain can be represented as a deterministic transformation $g([\mathbf{x}, \mathbf{y}]) = [\mathbf{y}, \mathbf{x}]$, where the current and proposed states are swapped. This swapping of states preserves the first coordinate as the state of the chain. Since this transformation is simply a permutation of variables, the Jacobian of the continuous component of the transformation is 1 in absolute value. We can verify that $\pi(\mathbf{x})$ is a marginal distribution of $\tilde{\pi}(\tilde{\mathbf{x}})$. By definition, $T(\mathbf{y}|\mathbf{x})$ is a probability function, so integrating $\tilde{\pi}$ over \mathbf{y} gives $\pi(\mathbf{x})$. Finally, the ratio $r(\tilde{\mathbf{x}})$ is computed as

$$r(\tilde{\mathbf{x}}) = \frac{\tilde{\pi}(g(\tilde{\mathbf{x}}))}{\tilde{\pi}(\tilde{\mathbf{x}})} |J(g_C(\tilde{\mathbf{x}}))| = \frac{\pi(\mathbf{y})T(\mathbf{x}|\mathbf{y})}{\pi(\mathbf{x})T(\mathbf{y}|\mathbf{x})}.$$

Therefore, we accept the proposal \mathbf{y} with probability $a(\mathbf{x}, \mathbf{y}) = 1 \wedge \frac{\pi(\mathbf{y})T(\mathbf{x}|\mathbf{y})}{\pi(\mathbf{x})T(\mathbf{y}|\mathbf{x})}$, which is the standard Metropolis-Hastings acceptance ratio. In the next section we apply this approach to derive a general acceptance probability formula for the MTM algorithm.

2.2 The multiple-try Metropolis acceptance probability

Suppose that π is a probability distribution over an arbitrary state-space \mathcal{X} . Multiple-try Metropolis is an iterative procedure that produces a sample from a Markov chain that has π as its stationary distribution [Liu et al., 2000]. In this section we first describe the MTM algorithm, then use the procedure described in Section 2.1 to derive an acceptance probability that will ensure the correct stationary distribution.

Consider an arbitrary iteration of the algorithm at state $\mathbf{x} \in \mathcal{X}$. The MTM algorithm obtains the next state in the chain by first drawing $M \geq 1$ candidates from M proposal distributions: $\mathbf{y}_m \sim T_m(\cdot|\mathbf{x})$, $m = 1, \dots, M$. One of these candidates is selected with probability $P(J|\mathbf{y}_{1:M}, \mathbf{x})$ for $J \in \{1, \dots, M\}$. Once the candidate $\mathbf{y} = \mathbf{y}_J$ is selected, “backwards samples” are generated:

$$\mathbf{x}_m^* \begin{cases} = \mathbf{x}, & \text{if } m = J, \\ \sim T_m(\cdot|\mathbf{y}), & \text{if } m \neq J. \end{cases}$$

Finally, the proposal \mathbf{y} is accepted with some probability, or rejected in which case the chain remains at the state \mathbf{x} . Next, we derive an acceptance probability that will guarantee that the Markov chain generated by this procedure admits π as its stationary distribution.

First, the augmented space is constructed from the variables defined in the procedure outlined above: $\tilde{\mathbf{x}} = [\mathbf{x}, \mathbf{y}_{1:M}, J, \mathbf{x}_{-J}^*]$, where $\mathbf{x}_{-J}^* = [\mathbf{x}_1^*, \dots, \mathbf{x}_{J-1}^*, \mathbf{x}_{J+1}^*, \dots, \mathbf{x}_M^*]$. Assuming that the chain is at its stationary distribution, the distribution of \mathbf{x} is $\pi(\mathbf{x})$. Then, to obtain the joint probability distribution over the augmented space, take the product of $\pi(\mathbf{x})$ and the conditional distributions used to generate the candidates, backwards samples, and selected index J :

$$\tilde{\pi}(\tilde{\mathbf{x}}) = \pi(\mathbf{x}) \left[\prod_{m=1}^M T_m(\mathbf{y}_m|\mathbf{x}) \right] p(J|\mathbf{y}_{1:M}, \mathbf{x}) \prod_{m \neq J} T_m(\mathbf{x}_m^*|\mathbf{y}_J).$$

The choice of the involution is similar to that used in the MH example: the selected \mathbf{y}_J and \mathbf{x} are swapped, along with the other candidate draws for their backwards counterpart, and the selected index is left unchanged. That is, $g(\tilde{\mathbf{x}}) = [\mathbf{y}_J, \mathbf{x}_{1:J-1}^*, \mathbf{x}, \mathbf{x}_{J+1:M}^*, J, \mathbf{y}_{-J}]$. As with MH, since this transformation involves only a permutation of variables, the Jacobian term is one in absolute value.

To show that the target distribution is a marginal of the extended distribution, we integrate or sum over all of the auxiliary random variables. First, we integrate over the joint distribution of \mathbf{x}_{-J}^* resulting from the $M - 1$ shadow samples:

$$\begin{aligned} \int_{\mathcal{X}^{M-1}} \tilde{\pi}(\tilde{\mathbf{x}}) d\mathbf{x}_{-J}^* &= \pi(\mathbf{x}) \left[\prod_{m=1}^M T_m(\mathbf{y}_m|\mathbf{x}) \right] p(J|\mathbf{y}_{1:M}, \mathbf{x}) \int_{\mathcal{X}^{M-1}} \prod_{m \neq J} T_m(\mathbf{x}_m^*|\mathbf{y}_J) d\mathbf{x}_{-J}^* \\ &= \pi(\mathbf{x}) \left[\prod_{m=1}^M T_m(\mathbf{y}_m|\mathbf{x}) \right] p(J|\mathbf{y}_{1:M}, \mathbf{x}). \end{aligned}$$

The distribution over the selected candidate, J , is summed over, leaving only the marginal distribution $\pi(\mathbf{x})$ and the joint distribution of the candidate samples:

$$\begin{aligned} \sum_{J=1}^M \left\{ \pi(\mathbf{x}) \left[\prod_{m=1}^M T_m(\mathbf{y}_m|\mathbf{x}) \right] p(J|\mathbf{y}_{1:M}, \mathbf{x}) \right\} &= \pi(\mathbf{x}) \left[\prod_{m=1}^M T_m(\mathbf{y}_m|\mathbf{x}) \right] \sum_{J=1}^M p(J|\mathbf{y}_{1:M}, \mathbf{x}) \\ &= \pi(\mathbf{x}) \left[\prod_{m=1}^M T_m(\mathbf{y}_m|\mathbf{x}) \right]. \end{aligned}$$

The joint candidate distribution is integrated over, leaving the desired marginal distribution:

$$\pi(\mathbf{x}) \int_{\mathcal{X}^M} \left[\prod_{m=1}^M T_m(\mathbf{y}_m|\mathbf{x}) \right] d\mathbf{y}_{1:M} = \pi(\mathbf{x}).$$

Now we derive the form of the acceptance probability for a general MTM algorithm based on Equation 1.

$$\begin{aligned} \frac{\tilde{\pi}(g(\tilde{\mathbf{x}}))}{\tilde{\pi}(\tilde{\mathbf{x}})} &= \frac{\pi(\mathbf{y}_J) \left[\prod_{m=1}^M T_m(\mathbf{x}_m^*|\mathbf{y}_J) \right] p(J|\mathbf{x}_{1:M}^*, \mathbf{y}_J) \prod_{m \neq J} T_m(\mathbf{y}_m|\mathbf{x})}{\pi(\mathbf{x}) \left[\prod_{m=1}^M T_m(\mathbf{y}_m|\mathbf{x}) \right] p(J|\mathbf{y}_{1:M}, \mathbf{x}) \prod_{m \neq J} T_m(\mathbf{x}_m^*|\mathbf{y}_J)} \\ &= \frac{\pi(\mathbf{y}_J) T_J(\mathbf{x}|\mathbf{y}_J) p(J|\mathbf{x}_{1:M}^*, \mathbf{y}_J)}{\pi(\mathbf{x}) T_J(\mathbf{y}_J|\mathbf{x}) p(J|\mathbf{y}_{1:M}, \mathbf{x})}. \end{aligned}$$

Therefore, the acceptance probability for MTM, as described at the beginning of this section, is

$$a(\tilde{\mathbf{x}}) = 1 \wedge \frac{\pi(\mathbf{y}_J) T_J(\mathbf{x}|\mathbf{y}_J) p(J|\mathbf{x}_{1:M}^*, \mathbf{y}_J)}{\pi(\mathbf{x}) T_J(\mathbf{y}_J|\mathbf{x}) p(J|\mathbf{y}_{1:M}, \mathbf{x})}. \quad (2)$$

This matches a general form for the acceptance probability of the MTM algorithm found in the literature [Pandolfi et al., 2014].

3 The construction of an MTM algorithm

When constructing an MTM algorithm, two core components must be specified, each offering a degree of flexibility. The first component is the proposal distribution, $T_m(\cdot|\mathbf{x})$, and the second is the form of the probability function for selecting the J -th candidate, $P(J|\mathbf{y}_{1:M}, \mathbf{x})$. An outline of the MTM algorithm is given in Algorithm 1 below.

Algorithm 1 Multiple-try Metropolis kernel

```

1: Input: (a) Target distribution  $\pi$ ; (b) current state vector  $\mathbf{x}$ .
2: Settings: (a) Number of candidates  $M$ ; (b) proposal distributions  $\{T_m\}$ ; (c) selection probability  $P(J|\cdot)$ .
3: for  $m \in \{1, \dots, M\}$  do
4:   Generate candidate  $\mathbf{y}_m \sim T_m(\cdot|\mathbf{x})$ .
5: end for
6: Sample  $J \in \{1, \dots, M\}$  with probability  $P(J|\mathbf{y}_{1:M}, \mathbf{x})$ .
7: Set  $\mathbf{y} = \mathbf{y}_J$ .
8: for  $m \in \{1, \dots, M\}$  do
9:   if  $m = J$  then
10:    Set  $\mathbf{x}_m^* = \mathbf{x}$ .
11:   else
12:    Generate reverse samples  $\mathbf{x}_m^* \sim T_m(\cdot|\mathbf{y})$ .
13:   end if
14: end for
15: Compute acceptance probability  $a$  given by Equation 2.
16: Sample  $U \sim \text{Unif}(0, 1)$ .
17: if  $U < a$  then
18:   Return  $\mathbf{y}$ .
19: else
20:   Return  $\mathbf{x}$ .
21: end if

```

3.1 The proposal distribution

The choice of proposal distribution dictates how the algorithm explores the state space. Most commonly, MTM is designed using random-walk proposals [Casarin et al., 2013, Fontaine and Béard, 2022, Gagnon et al., 2023, Liu et al., 2000, Pandolfi et al., 2014, Yang et al., 2019], typically of the form $\mathbf{y}_m \sim \mathcal{N}(\mathbf{x}, \Sigma_m)$. In addition to the parametric form of T_m , one must also determine the relationship between the proposal distribution and the index m . In the simplest case, set $\Sigma_j = \Sigma$ to obtain $\mathbf{y}_{1:M}$ as M independent draws from a common proposal distribution $T(\cdot|\mathbf{x})$ [Fontaine and Béard, 2022, Gagnon et al., 2023, Liu et al., 2000]. In general, each proposal distribution may be distinct such that the form of T_m does depend on the candidate index m . For example, to facilitate both local exploration while still permitting large jumps, one can set $\sigma_1 < \dots < \sigma_M$, in a univariate setting. The preceding discussion of the MTM algorithm has implicitly assumed that the \mathbf{y}_m 's are being generated by proposing over the full state vector. One can also obtain the next state in the chain by proposing each component of the state vector in a component-wise or block-wise fashion [Yang et al., 2019]. In a component-wise proposal, in a given iteration each component i is updated sequentially based on the proposal distributions $y_{i,m} \sim T_{i,m}(\cdot|x_i)$. This algorithm is outlined in Algorithm 2; the algorithm corresponding to a full vector proposal was that given in Algorithm 1. When each component update is performed in $\mathcal{O}(d)$ time, component-wise MH algorithms are expected to have greater per-iteration cost, although if these updates can be performed in $\mathcal{O}(1)$, then the theoretical computation time between a full and component-wise proposal are comparable.

One way to improve algorithm performance is by using an adaptive proposal distribution. In the context of MCMC algorithms, this usually refers to algorithms that update the proposal distribution while the algorithm is running based on the history of the chain or the local topography of the target distribution. This adaptation eliminates the need for time-consuming manual tuning of the MCMC algorithm parameters and can improve the algorithm efficiency by optimising the proposal distribution. A common adaptation strategy involves using a scaled estimate of the covariance of the target distribution in the proposal step [Andrieu and Thoms, 2008, Fontaine and Béard, 2022]. After an initial burn-in period of n_0 iterations without adaptation, the algorithm updates the proposal covariance Σ and the mean vector $\boldsymbol{\mu}$. The mean vector is only used to update Σ , not as the mean of the proposal distribution. To ensure a disappearing auto-correlation function, a learning rate of $\gamma(n) = n^{-0.6}$ is used to scale the change made to the proposal parameters

Algorithm 2 Component-wise Multiple-try Metropolis kernel

```

1: Input: (a) Target distribution  $\pi$ ; (b) current state vector  $\mathbf{x}$ .
2: Settings: (a) Number of candidates  $M$ ; (b) proposal distributions  $\{T_{i,m}\}$ ; (c) selection probability  $P(J|\cdot)$ .
3: for  $i \in \{1, \dots, d\}$  do
4:   for  $m \in \{1, \dots, M\}$  do
5:     Set  $\mathbf{y}_m = \mathbf{x}$ .
6:     Sample  $i$ -th element  $y_{i,m} \sim T_{i,m}(\cdot|x_i)$ .
7:   end for
8:   Sample  $J \in \{1, \dots, M\}$  with probability  $P(J|\mathbf{y}_{1:M}, \mathbf{x})$ .
9:   Set  $\mathbf{y} = \mathbf{y}_J$ .
10:  for  $m \in \{1, \dots, M\}$  do
11:    Set  $\mathbf{x}_m^* = \mathbf{x}$ .
12:    if  $m \neq J$  then
13:      Generate reverse samples  $x_{i,m}^* \sim T_{i,m}(\cdot|y_i)$ .
14:    end if
15:  end for
16:  Compute acceptance probability  $a$  given by Equation 2.
17:  if  $U \sim \text{Unif}(0, 1) < a$  then
18:    Update  $\mathbf{x} = \mathbf{y}$ .
19:  end if
20: end for
21: Return  $\mathbf{x}$ .

```

at each iteration [Fontaine and Béard, 2022]. This algorithm is described in Algorithm 3. The corresponding proposal distribution would be $\mathcal{N}(\mathbf{x}, \Sigma \times 2.38/\sqrt{d})$, where 2.38 is an optimal scaling parameter [Roberts et al., 1997].

Algorithm 3 Adaptive Metropolis

```

1: Input: (a) State  $\mathbf{x}$ ; (b) iteration  $n$ ; (c) proposal variance  $\Sigma$  and mean  $\boldsymbol{\mu}$ .
2: Settings:  $n_0 = 100$ .
3: if  $n \leq n_0$  then
4:   Return  $\Sigma, \boldsymbol{\mu}$ .
5: else
6:   Compute learning rate  $\gamma = n^{-0.6}$ .
7:   Update proposal covariance  $\Sigma = \Sigma + \gamma(\mathbf{x}_n - \boldsymbol{\mu})^T(\mathbf{x}_n - \boldsymbol{\mu})$ .
8:   Updating running mean  $\boldsymbol{\mu} = \boldsymbol{\mu} + \gamma(\mathbf{x}_n - \boldsymbol{\mu})$ .
9:   Return  $\Sigma, \boldsymbol{\mu}$ .
10: end if

```

Adaptation can also be done in a way that leverages the fact that the MTM algorithm can propose values under several different variances at each iteration. For example, consider a setting where we have a component-wise proposal and the $\sigma_{i,m}$'s are equally spaced on the \log_2 -scale. If candidates are only selected from low-variance or high-variance proposals, then the proposal distributions have not been efficiently specified. To determine the $\sigma_{i,m}$'s adaptively, periodically update the proposal variances such that candidates drawn from all proposal distributions have a reasonably well-balanced selection rate [Yang et al., 2019]. This scheme requires that the selection rate for each candidate be recorded, $S_{i,m}$ for $i = 1, \dots, d$ and $m = 1, \dots, M$. In order to ensure reasonable information can be collected on the selection rate, adaptation occurs only every β -th iteration. During an adaptation step, adaptation is performed with probability $P = \max(0.99^{a-1}, a^{-1/2})$, where $a = (n - \beta)/\beta$. If $\sigma_{i,M} > 2/M$, then $\sigma_{i,M}$ is doubled; if $\sigma_{i,M} < 1/(2M)$ and $\sigma_{i,M}/2 > \sigma_{i,1}$, then $\sigma_{i,M}$ is halved. Conversely, if $\sigma_{i,1} > 2/M$, then $\sigma_{i,1}$ is halved; if $\sigma_{i,1} < 1/(2M)$ and $2\sigma_{i,1} < \sigma_{i,M}$, then $\sigma_{i,1}$ is doubled. If $\sigma_{i,1}$ or $\sigma_{i,M}$ is changed, then the rest of the $\sigma_{i,m}$'s are updated so that they are equally spaced on the \log_2 scale. For practical reasons, a lower bound of 2^ϵ and an upper bound of 2^L are set on the $\sigma_{i,m}$'s. The pseudocode for this algorithm is given in Algorithm 4; a more rigorous discussion and analysis of this adaptation algorithm can be found in the original paper [Yang et al., 2019].

While this work focuses on single-chain MTM methods, multi-chain MTM algorithms can also be constructed. For example, one can have K simultaneous and interacting chains targeting the same distribution [Casarin et al., 2013]. In this formulation, the k -th chain is updated by drawing M proposals from $T_m^{(k)}(\cdot|\tilde{f}^{(k)}(\mathbf{x}))$. The function

Algorithm 4 Balanced Selection Rate

```

1: Input: (a) State  $\mathbf{x}$ ; (b) iteration  $n$ ; (c) current proposal variances  $\sigma_{i,m}$ 's.
2: Settings:  $\beta = 100$ ,  $\epsilon = -15$ ,  $L = 50$ .
3: Compute adaptation probability:  $a = (n - \beta)/\beta$ ,  $P = \max(0.99^{a-1}, a^{-1/2})$ .
4: Sample  $U \sim \text{Unif}(0, 1)$ .
5: if  $n \bmod \beta = 0$  and  $U < P$  then
6:   for  $i = 1, \dots, d$  do
7:     if  $S_{i,M} > 2/M$  then
8:        $\sigma_{i,M} = \min(2\sigma_{i,M}, 2^L)$ .
9:       Rescale  $\sigma_{i,1:M}$  to be equally spaced on the  $\log_2$ -scale.
10:    else if ( $S_{i,M} < 1/(2M)$ ) and ( $\sigma_{i,M}/2 > \sigma_{i,1}$ ) then
11:       $\sigma_{i,M} = \max(\sigma_{i,M}/2, 2^\epsilon)$ .
12:      Rescale  $\sigma_{i,1:M}$  to be equally spaced on the  $\log_2$ -scale.
13:    end if
14:    if  $S_{i,1} > 2/M$  then
15:       $\sigma_{i,1} = \max(\sigma_{i,1}/2, 2^\epsilon)$ .
16:      Readjust  $\sigma_{i,1:M}$  to be equally spaced on the  $\log_2$ -scale.
17:    else if ( $S_{i,1} < 1/(2M)$ ) and ( $2\sigma_{i,1} < \sigma_{i,M}$ ) then
18:       $\sigma_{i,1} = \min(2\sigma_{i,1}, 2^L)$ .
19:      Readjust  $\sigma_{i,1:M}$  to be equally spaced on the  $\log_2$ -scale.
20:    end if
21:  end for
22: end if
23: Return the  $\sigma_{i,m}$ 's.

```

$\tilde{f}^{(k)}(\mathbf{z}) = (\mathbf{x}^{(1:k-1)}, \mathbf{z}, \mathbf{x}^{(k+1:K)})^T$ takes the vector of current states across all K chains and swaps the argument for the current value of chain k . The form of \tilde{f} parses the chains and determines how they interact. This interacting-chain MTM algorithm has been discussed in detail elsewhere [Casarin et al., 2013]. A more general framework for multi-chain MTM algorithms has been left to a later work.

3.2 The candidate selection probability

While acceptance probability derived in Section 2.2 does not suggest a particular form for the selection probability $P(J|\mathbf{y}_{1:M}, \mathbf{x})$, the existing literature on MTM methods have used a weight-based approach to sampling candidates. In particular, a weight function $u_m(\mathbf{y}_m, \mathbf{x})$ is defined so that each candidate and backward sample can be assigned a weight. The selection probability is then taken to be the normalized weight of a particular candidate

$$P(J|\mathbf{y}_{1:M}, \mathbf{x}) = \frac{u_J(\mathbf{y}_J, \mathbf{x})}{\sum_{m=1}^M u_m(\mathbf{y}_m, \mathbf{x})}. \quad (3)$$

The remainder of this section will focus on the form of the weight function.

In general, $u_m(\mathbf{y}_m, \mathbf{x})$ needs only be positive on the support of π [Pandolfi et al., 2014]. Some authors prefer a more restricted form for the weight function [Liu et al., 2000]:

$$u_m(\mathbf{y}_m, \mathbf{x}) = \pi(\mathbf{y}_m)T_m(\mathbf{x}|\mathbf{y}_m)\lambda(\mathbf{y}_m, \mathbf{x}), \quad (4)$$

where the scaling function $\lambda(\mathbf{y}_m, \mathbf{x})$ is positive on the support of π and is symmetric about $(\mathbf{y}_m, \mathbf{x})$. Substituting the restricted weight function into Equation 2 gives us:

$$a(\tilde{\mathbf{x}}) = 1 \wedge \frac{\sum_{m=1}^M u_m(\mathbf{y}_m, \mathbf{x})}{\sum_{m=1}^M u_m(\mathbf{x}_m^*, \mathbf{y})}. \quad (5)$$

A constant scaling function such as $\lambda \equiv 1$ is a valid form for the scaling function [Liu et al., 2000] and results in $u_m(\mathbf{y}_m, \mathbf{x}) = \pi(\mathbf{y}_m)T(\mathbf{x}, \mathbf{y}_m)$, the joint distribution of $(\mathbf{y}_m, \mathbf{x})$. Two examples of a non-constant scaling function are

$$\lambda(\mathbf{y}_m, \mathbf{x}) = \left(\frac{T(\mathbf{y}_m|\mathbf{x}) + T(\mathbf{x}|\mathbf{y}_m)}{2} \right)^{-1} \quad [\text{Liu et al., 2000}] \quad (6)$$

and

$$\lambda(\mathbf{y}_m, \mathbf{x}) = [T_m(\mathbf{x}|\mathbf{y}_m)T_m(\mathbf{y}_m|\mathbf{x})]^{-\rho} \quad [\text{Liu et al., 2000}], \quad (7)$$

where ρ is a tuning parameter. Both scaling functions satisfy the symmetry condition, regardless of the form of the proposal distribution. If $T(\mathbf{y}_m|\mathbf{x})$ is a symmetric proposal, then the weight function corresponding to Equation 6 simplifies to $u_m(\mathbf{y}_m, \mathbf{x}) = \pi(\mathbf{y}_m)$. Since in this case candidate m is selected with probability proportional to its density under the target distribution, this is called the ‘‘proportional’’ weight function. In Equation 7, if $\rho = 1$ then the weight simplifies to $u_m(\mathbf{y}_m, \mathbf{x})$. This is called the ‘‘importance’’ weight function since sampling from candidates with weights of this form is analogous to importance sampling. A fourth version of the scaling parameter is

$$\lambda(\mathbf{y}_m, \mathbf{x}) = T_m(\mathbf{y}_m|\mathbf{x})^{-1} \|\mathbf{y}_m - \mathbf{x}\|^\alpha \quad [\text{Yang et al., 2019}], \quad (8)$$

where α is a tuning parameter and T_m is a symmetric proposal distribution. By incorporating the distance between the candidates and the current state of the chain in this way, of two candidates that are similarly likely under π , the candidates which has a greater jump distance will be assigned more weight. In this way, the form of the weight function promotes exploration by encouraging larger jumps at each step. For this reason it is called the ‘‘jump distance’’ weight function. Empirical evidence suggests an optimal range for α to be $\alpha \in (2, 4)$ [Yang et al., 2019].

Using the general form of the weight function, one can define a weight function that has good theoretical qualities. By using the weight function of the form

$$u_m(\mathbf{y}_m, \mathbf{x}) = \sqrt{\pi(\mathbf{y}_m)},$$

it has been shown that the algorithm has fast convergence times [Gagnon et al., 2023]. Additionally, using a single proposal distribution and this weight function results in an MTM kernel that approximates that of Hamiltonian Monte Carlo as $M \rightarrow \infty$. The five weight functions addressed thus far have been summarized in Table 1.

Weight function	Functional form	Source
Constant	$\pi(\mathbf{y}_m)T(\mathbf{x} \mathbf{y}_m)$	Liu et al. [2000]
Importance	$\pi(\mathbf{y}_m)/T(\mathbf{y}_m \mathbf{x})$	Liu et al. [2000]
Proportional	$\pi(\mathbf{y}_m)$	Liu et al. [2000]
Locally balanced	$\sqrt{\pi(\mathbf{y}_m)}$	Gagnon et al. [2023]
Jump distance	$\pi(\mathbf{y})\ \mathbf{y}_m - \mathbf{x}\ ^\alpha$	Yang et al. [2019]

Table 1: Weight functions discussed in Section 3, specified in the form $u_m(\mathbf{y}_m, \mathbf{x})$.

An alternative use of the general form of the weight function is to construct an approximate MCMC method that exchanges exactness for reduced computation time. Computing the acceptance probability in Equation 5 requires the evaluation of the target distribution $2M$ times. To reduce the computational burden of the multiple-try framework, one can use a Taylor expansion of the target distribution around the current state of the chain [Pandolfi et al., 2014]:

$$\begin{aligned} \pi^*(\mathbf{y}_m, \mathbf{x}) &= \pi(\mathbf{x})B(\mathbf{y}_m, \mathbf{x}), \\ B(\mathbf{y}_m, \mathbf{x}) &= \exp \left[s(\mathbf{x})'(\mathbf{y}_m - \mathbf{x}) + \frac{1}{2}(\mathbf{y}_m - \mathbf{x})'D(\mathbf{x})(\mathbf{y}_m - \mathbf{x}) \right], \\ u_m^*(\mathbf{y}_m, \mathbf{x}) &= \pi^*(\mathbf{y}_m)T_m(\mathbf{y}_m|\mathbf{x})\lambda(\mathbf{y}_m, \mathbf{x}), \end{aligned}$$

where s and D are the gradient and Hessian of $\log \pi(\mathbf{x})$ with respect to \mathbf{x} . By designing the weight function in this way, the target distribution need only be evaluated at the current state \mathbf{x} and at the proposal \mathbf{y}_J , rather than at each of the \mathbf{y}_m ’s and \mathbf{x}_m^* ’s. However, by using π^* in the weight function, the stationary distribution of the algorithm will be π^* rather than π .

4 Simulation experiments

The subsequent simulation experiments are organized into three categories, based on the type of target distribution they represent: those exhibiting non-Gaussian characteristics, multimodal distributions, and posterior distributions over parameters of interest. First, we describe the general set-up of all experiments, then the specifics of each experiment are given.

Common settings All experiments vary the weight function, proposal distribution, and number of candidate draws. The weight functions considered in the simulation study are the ‘‘proportional’’, ‘‘importance’’, ‘‘jump distance’’, and ‘‘locally balanced’’ weight functions, which are summarized in Table 1. The proposal distributions are described in

the following paragraph; an analysis of multi-chain MTM algorithms [Casarin et al., 2013] is left to future work. The configuration of the proposal distribution is defined by: 1) whether the M candidates are drawn from the same proposal distribution (Homogeneous) or different proposal distributions (Heterogeneous), and 2) proposing jointly over the full state space (Full) as in Algorithm 1 or proposing from the joint space in a component-wise fashion (CW) as in Algorithm 2. The four combinations of settings are the four proposal distribution configurations used in the experiments. In all four settings, a Gaussian random-walk kernel is used with an adaptive (co)variance. Both Homogeneous-Full and Heterogeneous-Full proposals use the Adaptive Metropolis procedure (Algorithm 3) [Fontaine and Béard, 2022, Haario et al., 1999], the Homogeneous-CW proposal uses the univariate version of the same algorithm, and the Heterogeneous-CW proposal uses the Balanced Selection Rate procedure (Algorithm 4) [Yang et al., 2019]. The range of values for number of candidates (M) varies between experiments. When $M = 1$, the MTM algorithm is equivalent to Metropolis-Hastings. All experiments use $M = 1$ as a baseline to evaluate the relative benefit gained by using multiple candidates. However, $M = 1$ is not used in the Heterogeneous-CW proposal configuration, as the adaptation scheme does not accommodate $M < 2$.

Computing resources For each experiment setting, 50 chains are generated by running the algorithm for a fixed time budget on an Intel Gold 6148 Skylake @ 2.4 GHz CPU; the running time varies between experiments. The implementation of the algorithms and the simulation study is done in Julia [Bezanson et al., 2017] with visualizations rendered in R [R Core Team, 2022] with the `ggplot2` package [Wickham, 2016]. The Julia code can be found here: <https://github.com/SFU-Stat-ML/multiple-try-metropolis-experiments>.

Post-processing Given the large number of chains being generated, manually determining burn-in is infeasible and setting a fixed proportion of samples as burn-in was found to be ineffective given the variable performance of the algorithms. To automatically determine a reasonable burn-in for each generated sample, we use the ad-hoc procedure described in Algorithm 5 in the Supplementary Materials which is designed to choose a burn-in period that corresponds to a stable mean estimate.

4.1 Non-Gaussian target distributions

In this simulation study we use the term “non-Gaussian” to refer to target distributions that are characterized by features that are difficult to approximate by a Gaussian distribution, except at very local scales. This is of interest here because the typical building block of the MTM compound proposal is a Gaussian random-walk proposal, perhaps with an adaptive proposal covariance. The MH algorithm with an adaptive proposal (equivalent to MTM with $M = 1$) can have difficulty with non-Gaussian target distributions because the locally optimal Gaussian random-walk kernel will have to explore the state space very slowly in order to ensure a reasonable acceptance rate. These simulations demonstrate how increasing M and/or using adaptation schemes unique to the MTM framework can allow MTM to overcome shortcomings of MH, as well as understand which algorithm configurations are best-suited to non-Gaussian target distributions.

Banana distribution The first target distribution exhibiting non-Gaussian features is the “banana distribution”, which is often used to analyze the performance of MCMC algorithms [Andrieu and Thoms, 2008, Biron-Lattes et al., 2024, Fontaine and Béard, 2022, Haario et al., 1999, Yang et al., 2019]. The distribution is defined as a transformation of an d -dimensional vector \mathbf{x} of standard Gaussian random variables that results in the following unnormalized probability density function:

$$\pi(\mathbf{x}) \propto \exp \left[-x_1^2/200 - \frac{1}{2} (x_2 + Bx_1^2 - 100B)^2 - \frac{1}{2} (x_3^2 + x_4^2 + \dots + x_d^2) \right].$$

The parameter B controls the degree of non-Gaussianity, such that π is more difficult to sample from as B increases. In our experiment we consider $\log_{10} B = -2, -1.75, \dots, -0.5$. The resulting distribution is unimodal with contours taking a crescent shape when jointly plotting (x_1, x_2) , making the first two coordinates the hardest to sample. Alternative parameterizations can result in multiple coordinate pairs having non-Gaussian curvature [Fontaine and Béard, 2022]. The experiment was run with $M = 1, 5, 10, 15, 20$ for each of the previously described weight and proposal distribution settings resulting in 560 different algorithm settings. To evaluate the sampling performance, we compute the multivariate effective sample size (mESS) [Vats et al., 2019] after running each algorithm for ten seconds and removing burn-in samples via Algorithm 5. Examples of the contours of the banana distribution are shown below in Figure 1.

With respect to the relative speeds of the algorithms, those using a full proposal were substantially faster than those using a component-wise proposal. This is within expectations, as our implementation of the component-wise proposal was not optimized for each target distribution. The difference between the Homogeneous-CW and Heterogeneous-CW proposals was insubstantial, while the Multiple-Full proposal was much slower than the Homogeneous-Full proposal. These findings were similar for all experiments.

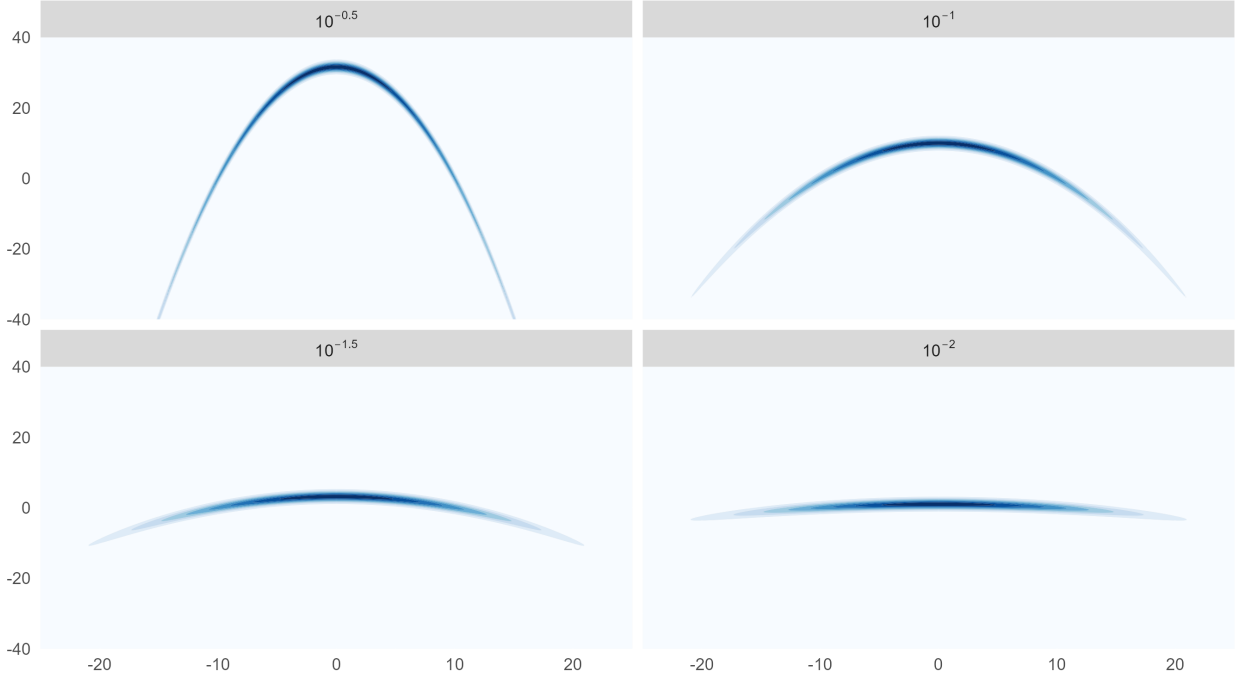


Figure 1: Contours for the banana distribution for non-Gaussianity parameters $\log_{10} B = -2, -1.5, -1, -0.5$.

The raw mESS generated with a fixed time budget under each algorithm setting are shown in Figure 2. The distribution of mESS over the 50 independent runs in each algorithm setting are visualised by computing the empirical median and 50% intervals. Comparing the results between $M = 1$ and $M > 1$ finds some improvement in all but the Heterogeneous-Full proposal configuration. Both Homogeneous proposals show a degradation in sampling efficiency for $M > 5$, while the Heterogeneous-CW proposal is stable until $M > 10$. There is little observable impact from the choice of weight function. These patterns remain fairly consistent as the degree of non-Gaussianity increases.

In Figure 3 the mESS per iteration is shown for each algorithm setting. This plot shows the marginal contribution to the total mESS obtained from a single iteration of each algorithm. Compared to Figure 2, this indicates performance in an ideal setting where parallel computing regimes can be used to evaluate the weights and component-wise updates have been optimized. All combinations of weight function and proposal distribution show an increase in the per-iteration mESS gain when the number of candidates is increased. The component-wise proposals show better per-iteration sampling efficiency than the full proposals; the Homogeneous-CW proposal underperforming relative to the Heterogeneous-CW proposal. In all cases, the marginal increase in gains by increasing M is greater when degree of non-Gaussianity is lower. There does not appear to be a significant effect due to the choice of weight function.

Neal’s funnel Neal’s funnel distribution is a $(d + 1)$ -dimensional distribution such that the variance of the latter d dimensions scale exponentially with the first marginal distribution, resulting in a funnel-shaped distribution that presents a challenging target distribution for modern sampling algorithms [Neal, 2003, Biron-Lattes et al., 2024, Modi et al., 2024]. It is specified as following

$$y \sim \mathcal{N}(0, 3^2), \quad x_i \sim \mathcal{N}\left(0, \left[e^{y/\beta}\right]^2\right),$$

for $i = 1, \dots, d$, where β is a scale parameter that can be used to control the degree of non-Gaussianity. In our experiment we consider the following settings for β : $\log_{10} \beta^{-1} = [-0.5, -0.25, 0, 0.25, 0.5]$. Each algorithm setting is run with $M = 1, 5, 10, 15, 20$, resulting in 400 experiment settings, each run for ten seconds and with burn-in determined by Algorithm 5. For this target, performance is evaluated by comparing the empirical mean of y , the first marginal distribution, against its true mean.

The mean of the first marginal distribution of Neal’s funnel are shown in Figure 4. The scale of the Monte Carlo error using the Heterogeneous-CW proposal configuration is much smaller than that of the other configurations, so these

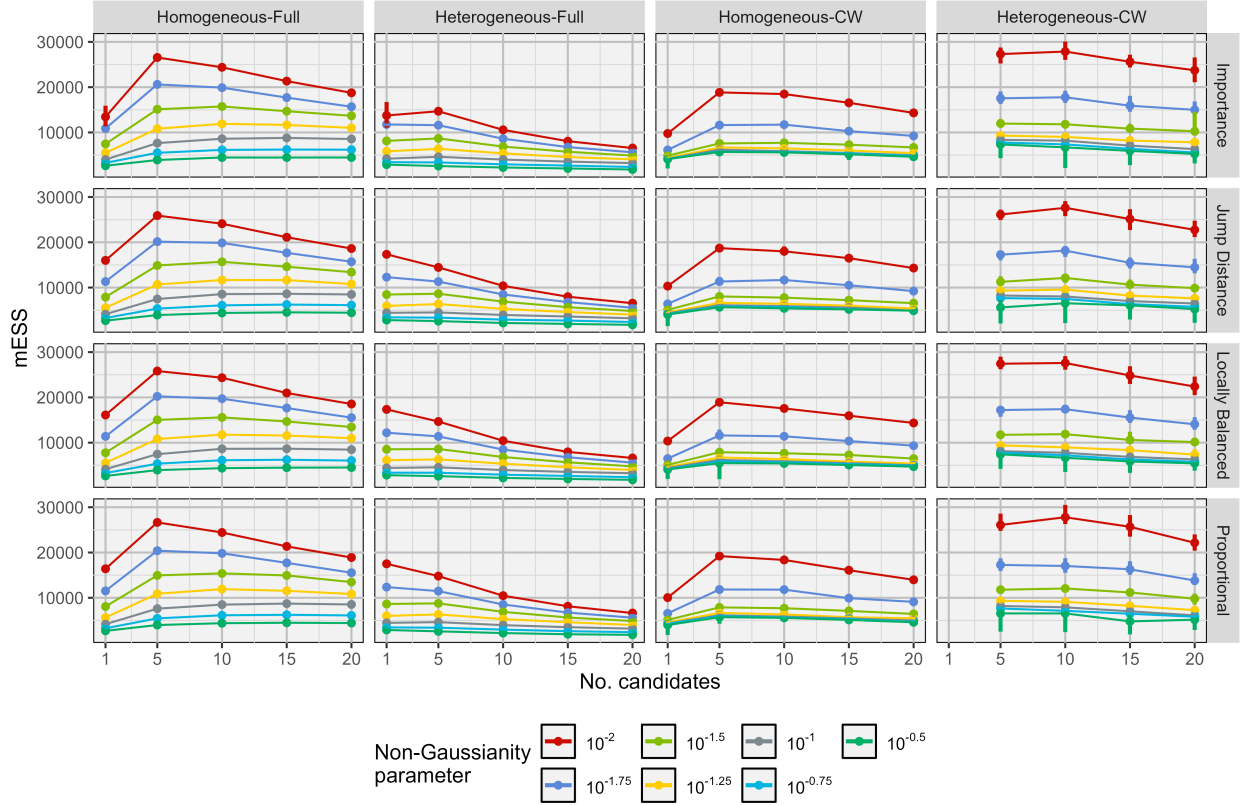


Figure 2: Raw mESS for the banana distribution. The median (point) and 50% interval (vertical line) over 50 independent runs are shown for each setting. Columns correspond to the proposal distribution configuration and rows to the weight function.

results are shown again separately in Figure 5. The estimate of the mean of the first marginal tends to be biased when the degree of non-Gaussianity is high, $\beta^{-1} > 1$, but increasing the number of candidates tends to reduce this bias. The Heterogeneous-CW proposal configuration shows fairly consistent Monte Carlo error with respect to M , for a given scale parameter; the other three proposals show a steep increase in the error for $M \geq 15$. While the Heterogeneous-CW proposal shows much lower bias and error than the other proposals, the 50% interval of mean estimates rarely captures the true mean for $\beta^{-1} > 1$; the other proposals do capture the true mean in the respective intervals for $M \geq 15$.

4.2 Multimodal target distribution

Sampling from multiple modes within a single MCMC sample is a persistently difficult task for Monte Carlo methods, so the second experiment evaluates the algorithms' ability to sample from a multimodal target distribution. It is common to use a Gaussian mixture distribution to assess algorithm performance in the presence of multimodality [Fontaine and Béard, 2022, Modi et al., 2024, Yang et al., 2019]. To do so a five-component Gaussian mixture distribution is used as the target distribution. For a d -dimensional distribution the component means are $\mathbf{0}_d$, $\mathbf{3}_d$, $-\mathbf{3}_d$, $[3, -3, 3, \dots]_d$, and $[-3, 3, -3, \dots]_d$; each component distribution has unit covariance matrix and the weight vector for the five components is $[1, 2, 4, 2, 1]$. When the target distribution is multimodal, it is important to sample from all modes and not just identify local maxima. Therefore, in order to assess the performance, a baseline sample is generated directly from the target distribution, then the two-sample Kolmogorov-Smirnov distance (KSD) is computed between each of the algorithm-generated samples and the baseline sample. This experiment was run with $M = 1, 5, 10, 15, 20$ and $d = 2, 4, 6, 8, 10$. Combined with the weight function and proposal distribution settings results in 400 experiment settings, each run for 30 seconds. Since the posterior samples are expected to be multimodal, the automatic burn-in procedure in Algorithm 5 is not suitable. Instead, we compute the KSD for each sample using a burn-in of 25%, 50%, and 75% of the generated samples and take the best result.

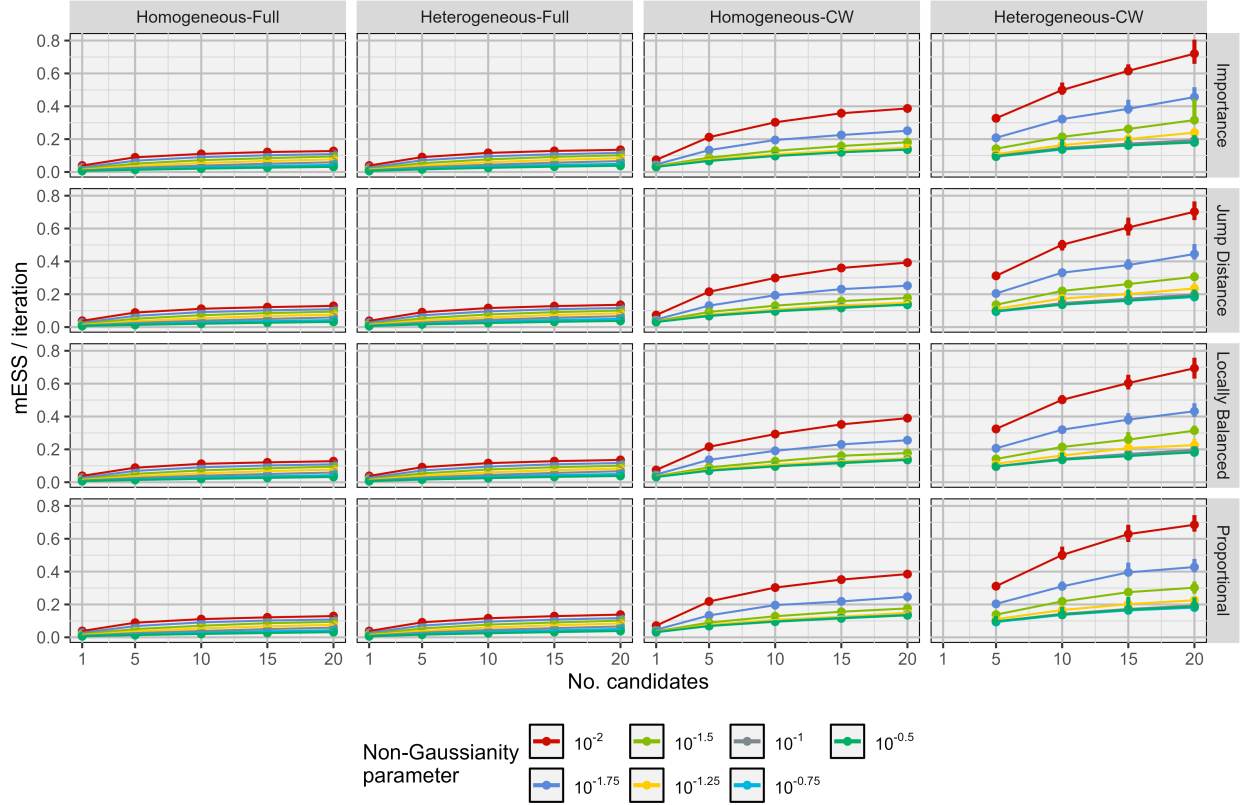


Figure 3: mESS per iteration for the banana distribution. The median (points) and 50% interval (vertical lines) over 50 independent runs are shown for each setting. Columns correspond to the proposal distribution configuration and rows to the weight function.

The KSD for each simulation setting are shown in Figure 6. The distribution of KSD over 50 independent runs under each setting is visualised by computing the empirical median, as well as the 50% and 90% intervals. In the 2-dimensional case, all settings show similar performance. When the dimension increases to 2 and 4, the component-wise proposals have a slightly higher median KSD than the full proposals, though the variance across runs is much higher. The 8-dimensional problem shows a distinct decrease in performance for the Homogeneous-CW proposal and a moderate decrease for the Heterogeneous-CW proposal. The full proposals show a small increase in median performance by increasing M above 1, though by $M = 10$ or $M = 15$ the variability in performance overlaps substantially with the component-wise proposals. All algorithm settings perform poorly in the 10-dimensional setting, with the full proposals showing some runs having good performance. There is no clear pattern with respect to the choice of weight function.

4.3 Parameter estimation

The final three target distributions are all posterior distributions over unknown model parameters, using the Monte Carlo estimate of the posterior mean as the point estimate for all of the parameters. Since this study is exploring the efficacy of Monte Carlo methods, rather than comparing the posterior means to true or baseline values, we estimate the Monte Carlo standard error associated with each algorithm configuration. The first posterior distribution is based on simulation and the remaining two are posteriors arising from real data problems.

Bayesian regression This target distribution is constructed from a simulated dataset, where the data is generated from the following regression model

$$y_i = \beta_0 + \boldsymbol{\beta}^T \mathbf{x}_i + \epsilon_i, \quad \epsilon_i \sim \mathcal{N}(0, \sigma^2), \quad (9)$$

where \mathbf{x}_i is a d -dimensional vector of predictor variables, β_0 is an intercept, $\boldsymbol{\beta}$ is a d -dimensional vector of regression coefficients, and σ is the observation noise. A sample of 1,000 data are simulated from this model with $\beta_0 = 1$,

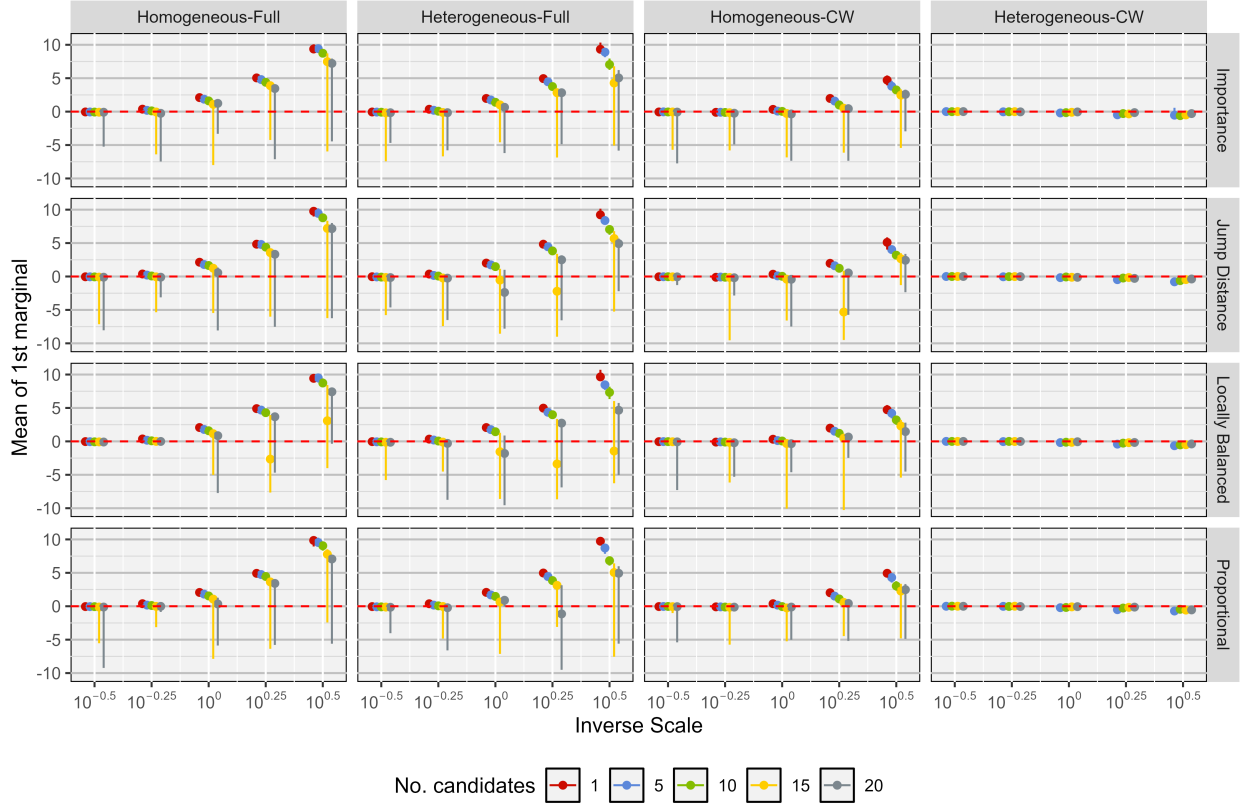


Figure 4: Empirical mean of the first marginal of Neal’s funnel distribution. Points represent the median and vertical lines the 50% interval of 50 independent runs under each setting. Columns correspond to the proposal distribution configuration and rows to the weight function.

$\beta^T = (0.1, 5, -5, 10)$, and $\sigma = 0.5$. The target distribution is the posterior distribution over these six parameters is constructed by taking the likelihood to be the same as the generating distribution (Equation 9), a Gaussian prior with mean 0 and standard deviation 100 for each of the five regression coefficients, and an inverse gamma prior with mean 1 and variance 100 is placed on σ . In addition to the weight function and proposal distribution settings outlined above, this experiment considers $M = 1, 2, 4, 6, 8, 10$, giving a total of 96 algorithm settings. To evaluate the Monte Carlo standard error (MCSE) under each setting, 10 datasets are generated and 50 chains are generated under each algorithm setting. Each algorithm is run for 90 seconds. The posterior mean is computed for each chain and the standard deviation of these posterior means is computed. The result is 10 samples of MCSE with respect to the data generative distribution for each setting.

The median of the 10 MCSEs is shown in Figure 7 for all estimated parameters. The Monte Carlo error produced by the full proposals is much lower than the component-wise proposals. For the component-wise methods, the lowest Monte Carlo error is achieved with 2 candidate draws and tends to either increase or remain constant as more candidate draws are used. As the Monte Carlo error increases, the variability in median MCSE between weight functions tends to increase, as can be seen in the results for the component-wise proposals.

To better compare algorithm settings, the MCSE for each of the ten random seeds used to generate the datasets, along with the corresponding medians, are for each method separately in Figures 12-15 in Appendix ???. For all proposal configurations, $M = 2$ tended to have the best performance, with error tending to increase as the number of candidates increases. Since $M = 2$ was good setting for all proposal distributions and weight functions are shown in Figure 8. The performance of the two full proposals are very similar; the performance of the two component-wise proposals are also similar to each other although the Heterogeneous-CW proposal exhibits greater variability in median MCSE than its Homogeneous-CW proposal counterpart. The relative performance of the methods is consistent between the intercept and regression parameters while for the noise parameter,

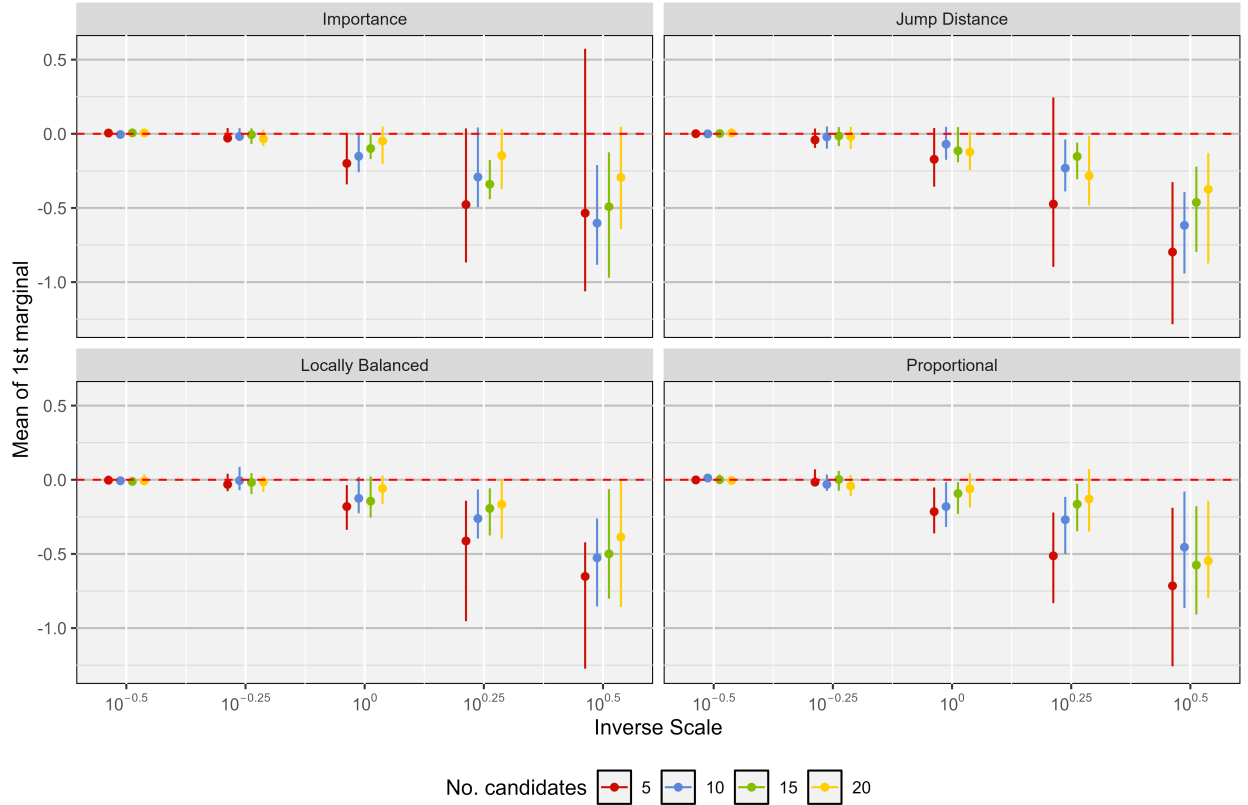


Figure 5: Empirical mean of the first marginal of Neal’s funnel distribution for the Heterogeneous-CW proposal configuration; points represent the median and vertical lines the 50% interval over the 50 independent runs. Each panel corresponds to a different weight function.

the median MCSE of the Heterogeneous-CW proposal is closer to that of the Full proposals, though with greater variability between datasets. There is no clear pattern associated with the weight function.

For the remaining two posteriors, some small proportion of the runs did not appear to converge, or converged to a point drastically different from the others. As a part of the post-processing, any results whose posterior mean was less than 1.5 times the interquartile range below the first quartile or more than 1.5 times the interquartile range above the third quartile were discarded from the analysis. For any given algorithm setting, the maximum number of runs discarded as outliers across all data problems was six.

Gull’s lighthouse Gull’s lighthouse problem [Gull, 1988] has been used to examine small sample size problems [Modi et al., 2024]. In this experiment, a boat observes flashes from a lighthouse that is located at position x_0 along the coastline at a distance y from the boat. Three flashes are observed $[x_1, x_2, x_3]$. The likelihood of x_i , given x_0 and y is $L(x_i|x_0, y) = \frac{y}{\pi(y^2 + (x_i - x_0)^2)}$, which is the probability density function of a Cauchy(x_0, y) distribution at x_i . Assuming improper uniform priors on x_0 and y gives the posterior distribution

$$\pi(x_0, y|x_1, x_2, x_3) \propto \prod_{i=1}^3 \text{Cauchy}(x_i|x_0, y),$$

which is our target distribution for this experiment. The experiment was run with $M = 1, 10, 20, \dots, 50$ candidate draws for a total of 96 settings; each setting was run for twenty seconds and the burn-in was computed using Algorithm 5.

The Monte Carlo distribution of the posterior means for the lighthouse problem are shown in Figure 9. For both position (x_0) and distance (y), the component-wise proposals provided consistent estimates across all weight functions and number of candidates; for distance, some increase in the width of the 95% intervals is observed in both of these

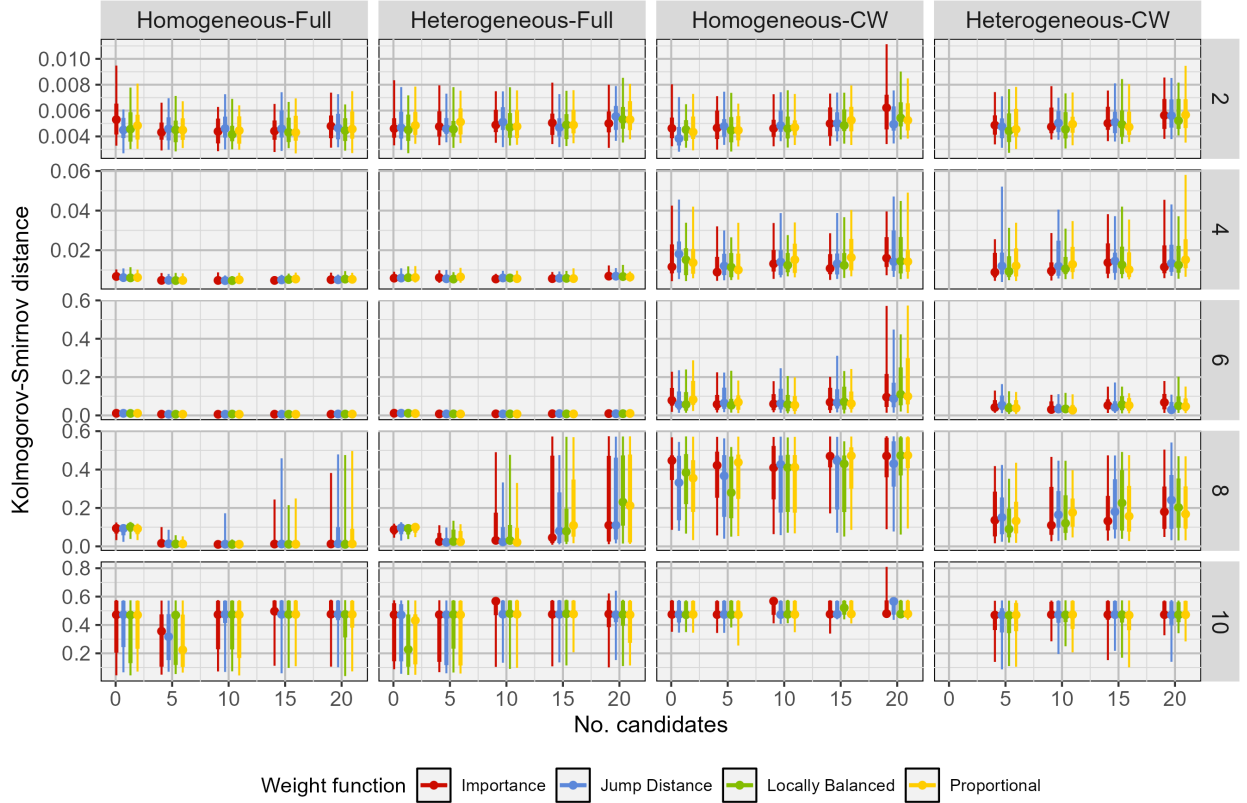


Figure 6: Kolmogorov-Smirnov distance between MTM samples and a sample directly from the target distribution. Distribution over 50 independent runs under each setting shown with the empirical median (points), 50% interval (thick lines) and 90% interval (thin lines). Columns correspond to the proposal distribution configuration and rows to the dimension of the target distribution.

proposals as the number of candidates increases. The full proposals exhibited more adverse behaviour, in particular, the posterior mean varies with the number of candidates. The MH setting is consistent with the component-wise estimates, but as the number of candidates increase there is a pattern of change in the point estimates; increasing in the position corresponding to a decrease in the distance. The position estimates are similar between the Homogeneous-Full and Heterogeneous-Full proposals; while there are differences in the distance point estimates between the two, there is little evidence of a statistically significant difference.

Eight schools The eight schools problem is a commonly used example of a Bayesian hierarchical model [Gelman et al., 2013]. This problem arises from a meta-analysis of the effect of preparation for a test in eight schools [Rubin, 1981]. For each of the eight schools an effect y_i its standard deviation σ_i were estimated. Each effect is assumed to have a Gaussian distribution with a school-specific mean θ_i and standard deviation σ_i . These school-specific means have a common hyperprior distribution with mean μ and standard deviation τ . The target distribution for this problem is taken as the posterior distribution arising from the Bayesian model specified below [Gelman et al., 2013]:

$$\begin{aligned} \mu &\sim \mathcal{N}(0, 5^2), & \tau &\sim \text{Cauchy}_+(0, 5), \\ \theta_i &\sim \mathcal{N}(\mu, \tau^2), & y_i &\sim \mathcal{N}(\theta_i, \sigma_i^2), \end{aligned}$$

for $i = 1, \dots, 8$. Each weight function and proposal configuration was run with $M = 1, 5, 10, 15, 20$ for a total of 80 experiment settings run for 45 seconds.

The MCSEs of the posterior mean for each parameter in the eight school model are shown in Figure 10. Component-wise proposals show a similar level of variability for all parameters with little observable impact of weight function. The full proposals tend to produce estimates with consistently lower variability than those of the component-wise proposals, with the clear exception of τ , the standard deviation of the school-specific means, and in some instances θ_1 and θ_7 . In

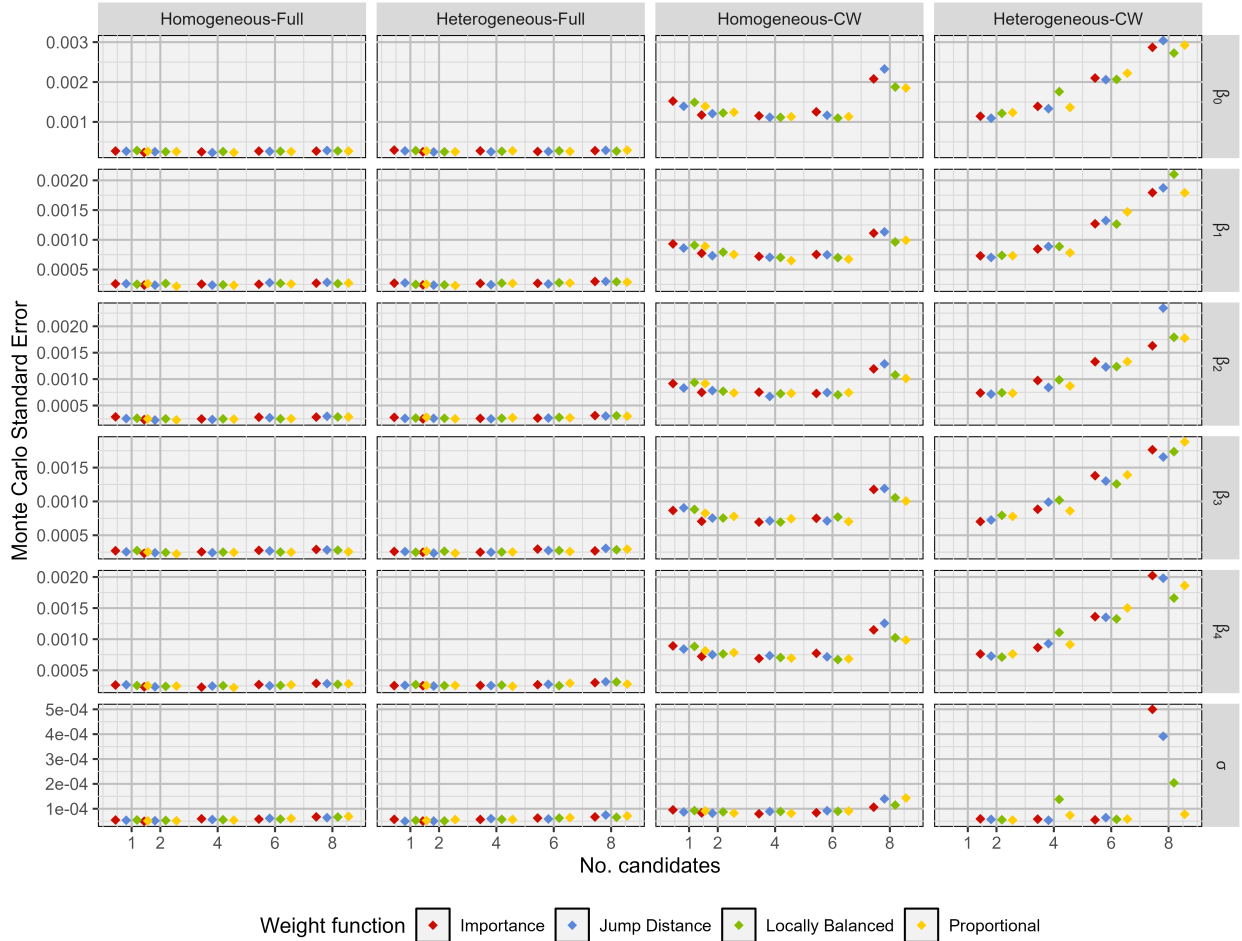


Figure 7: Monte Carlo standard error of mean of the Bayesian regression posterior. Points are the median over 50 independent runs for 10 randomly generated datasets. Columns correspond to the proposal distribution configuration and rows to the parameter being estimated.

most settings there is a small increase in MCSE resulting from an increase in the number of candidate proposals with this pattern being most clearly seen in the MCSEs for τ .

5 Discussion

The multiple-try Metropolis algorithm [Liu et al., 2000] is an extension of the Metropolis-Hastings algorithm that creates a compound proposal mechanism by drawing multiple candidates from a proposal distribution. In this paper we framed several extensions of the MTM algorithm within a single framework and evaluated the relative impact of different configurations on the performance of the algorithm.

A procedure for deriving acceptance probabilities for reversible MCMC algorithms was presented in Section 2, motivated by a deterministic Metropolis algorithm. Given a proposal distribution, the procedure outlined in Section 2.1 can be used to compute an acceptance probability that will result in a reversible MCMC algorithm with the correct target distribution. This has a wide range of application for constructing novel MCMC algorithms. This method was demonstrated on the MTM algorithm, providing a general framework within which extensions of the algorithm can be viewed.

In Section 3, we presented a unified framework for MTM algorithms. There is much flexibility in the design of an MTM algorithm, which can be used to adapt the algorithm to the particular needs of an analyst. The choice of proposal distribution and the form of the candidate selection probability, typically controlled through the weight function, were

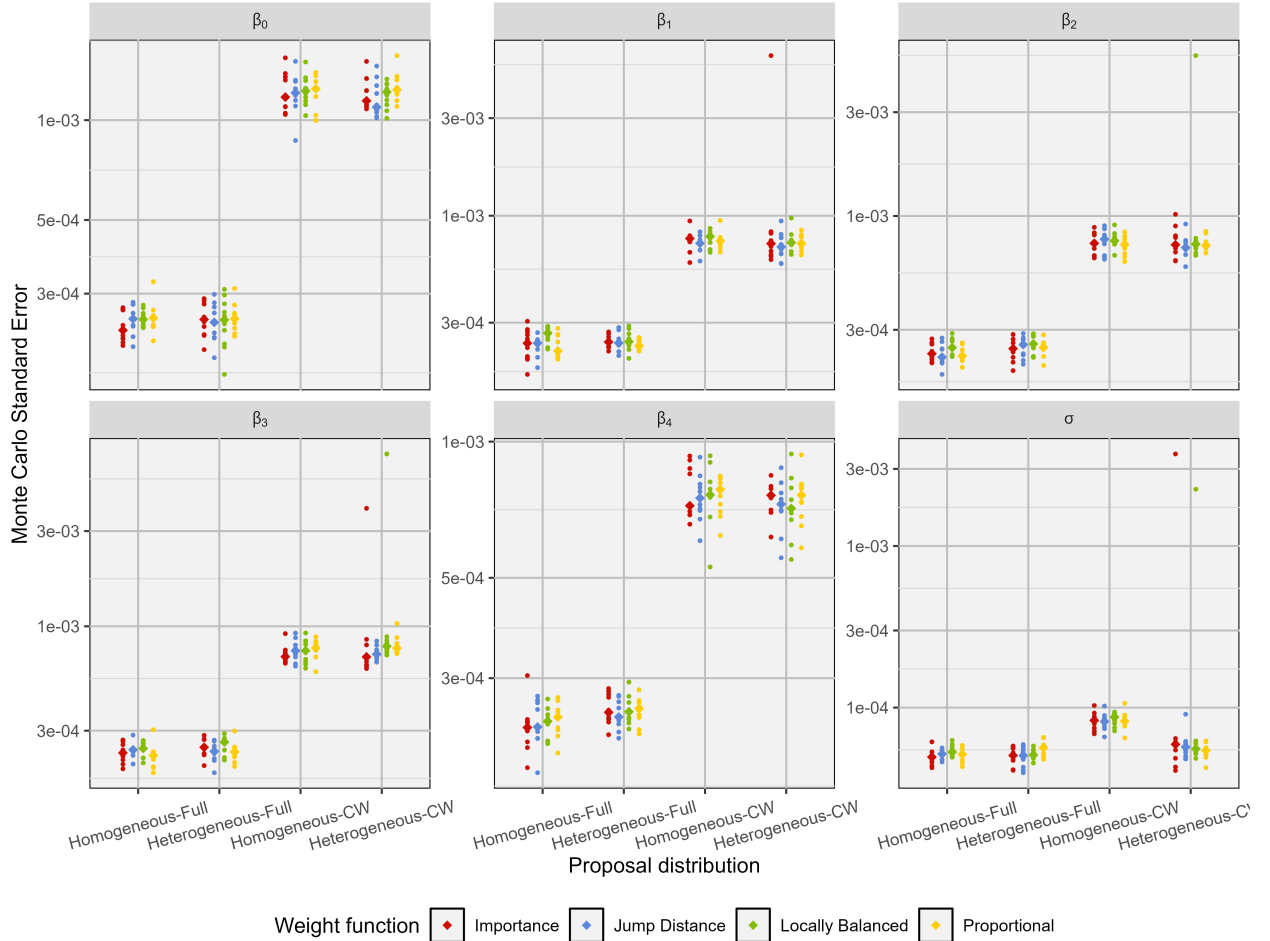


Figure 8: Monte Carlo standard error of mean of the Bayesian regression posterior for $M = 2$ candidates. Points are MCSE over 50 independent runs for 10 randomly generated datasets.

identified as the core components of the MTM algorithm through which the customization of the algorithm takes place; we elaborated on several examples of proposal distribution [Casarin et al., 2013, Fontaine and Béard, 2022, Liu et al., 2000, Yang et al., 2019] and weight function [Gagnon et al., 2023, Liu et al., 2000, Pandolfi et al., 2014, Yang et al., 2019] present in the academic literature.

Several simulation experiments were performed in Section 4 in which each experiment implemented a full factorial design to comprehensively explore the impact of the proposal distribution configuration, weight function, and the number of candidate draws. Using a component-wise proposal distribution with a Balanced Selection adaptation scheme produced the most effective sampler for the two non-Gaussian targets, both in terms of per-second and per-iteration effective sample size gain, as well as in the accuracy of estimating the mean of the distribution. On the other hand, in the presence of multimodality, using a component-wise proposal led to increased difficulty in navigating between modes, relative to its full proposal counterparts. In terms of Monte Carlo error, the results offered a less clear message. In a simple Bayesian regression setting, where the posterior distribution is Gaussian, the full proposals out-performed the component-wise proposals in terms of MCSE as well as the stability of MCSE with respect to the number of candidates. However, in the small-sample problem, the point estimates produced using the full proposals depended on the number of candidates, while the component-wise proposals were consistent. The eight schools problem, which exhibits some funnel-like characteristics, all proposals were fairly consistent with respect to the mean parameters, with the full proposals having lower MCSE. However, with respect to the variance parameter, the full proposals showed much higher MCSE while the component-wise proposals showed no difference.

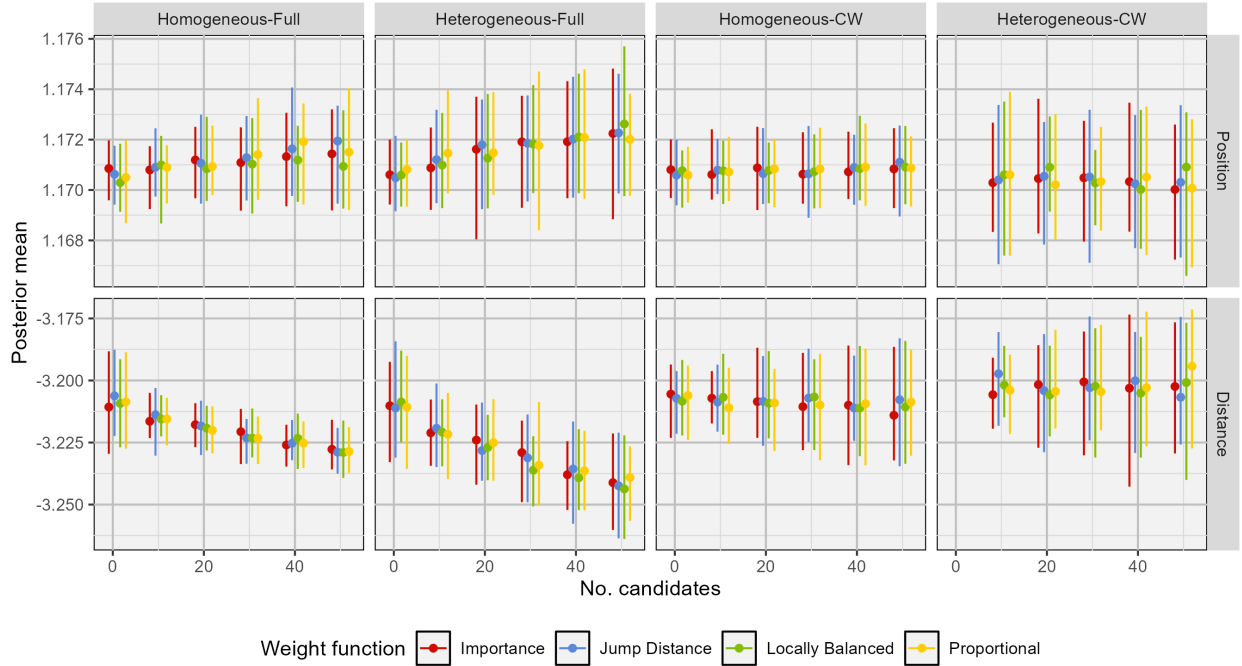


Figure 9: Posterior mean of the position (x_0) and distance (y) in Gull’s lighthouse problem. Points represent the median and vertical lines the 95% interval over the 50 independent runs. Columns correspond to the proposal distribution configuration.

In all experiments, the choice of the weight function had no clear impact. Much emphasis has been placed on developing the weight function in the literature, however novel weight functions are often accompanied by novelty in the configuration of the proposal distribution. However, our study suggests that the form of the weight function has less importance on the performance of the algorithm than the configuration of the proposal distribution or the number of candidate draws.

Limitations of the study The lack of evidence found to support importance of the weight function is surprising, given its relative prevalence in the MTM literature. Of particular note is the locally balanced weight function [Gagnon et al., 2023], which is well-motivated by theory. The theoretically driven discussions that motivate this weight function are primarily in terms of the convergence time. The design of our experiment focuses our analysis on the stationary performance of the algorithms, rather than their behaviour in the pre-stationary period. Therefore, we emphasize that our claims regarding the relative importance of the weight functions should be taken within this context.

Concluding remarks Multiple-try Metropolis is a flexible framework for designing algorithms, several aspects of which have been explored here. A component-wise proposal distribution, within the MTM framework, demonstrated good performance when sampling from non-Gaussian surfaces, as well as stable point estimates in some point estimation problems. In particular, the relatively poor performance of the component-wise proposals in the Bayesian regression problem relative to the more challenging posterior distributions may suggest that when designing an MTM algorithm, a full proposal is more suitable for distributions exhibiting Gaussian features and those deviating from Gaussianity would benefit from a component-wise proposal distribution. The framework presented in Section 2.1 provides a powerful tool for deriving novel MCMC algorithms.

Acknowledgements The authors would like to acknowledge funding from NSERC. Several discussions with Alexandre Bouchard-Côté were very helpful in developing the procedure outlined in Section 2.1 and in improving the clarity of the manuscript.

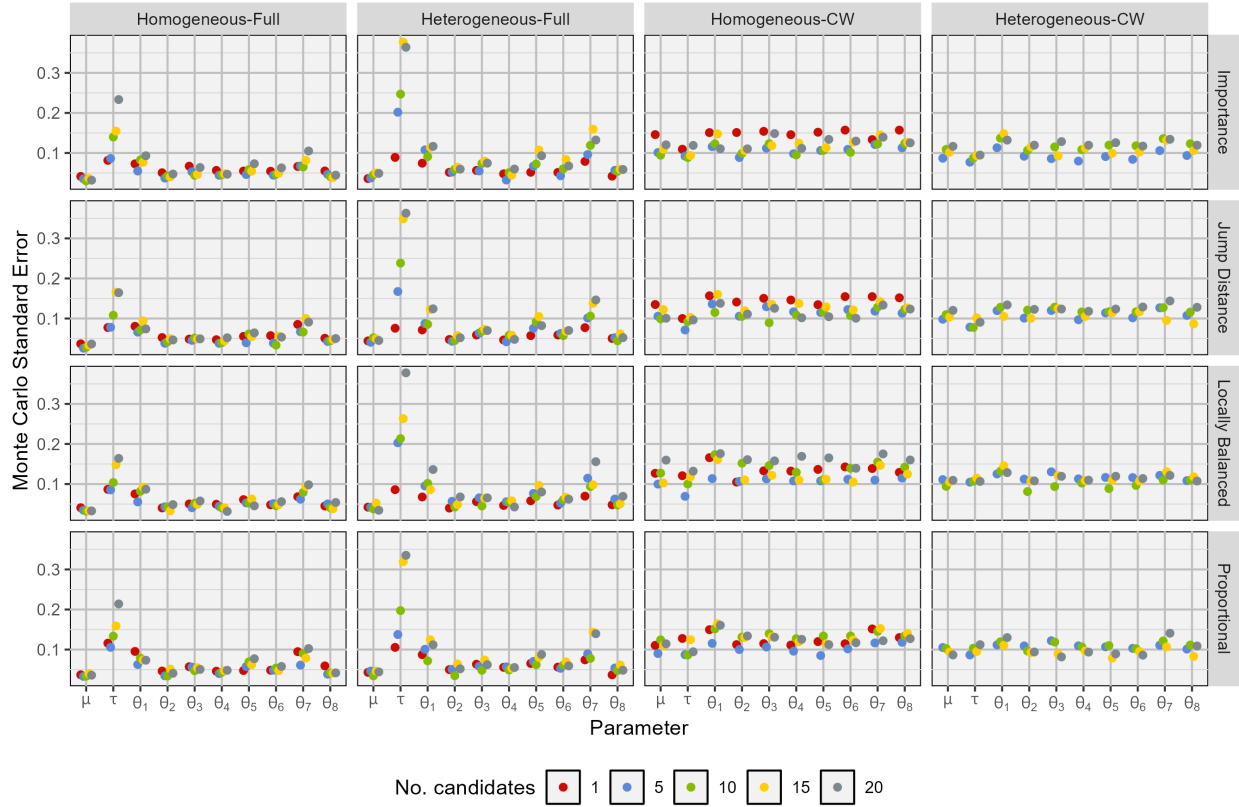


Figure 10: Median Monte Carlo standard error of the posterior mean for each parameter in the eight schools model. Columns indicate proposal distribution configuration and rows the weight function.

References

- W. K. Hastings. Monte Carlo sampling methods using Markov chains and their applications. *Biometrika*, 57(1):97–109, 1970.
- Nicholas Metropolis, Arianna W. Rosenbluth, Marshall Rosenbluth, Augusta H. Teller, and Edward Teller. Equation of state calculations by fast computing machines. *Journal of Chemical Physics*, 21:1087–1092, 1953.
- Jun S. Liu, Faming Liang, and Wing Hung Wong. The multiple-try method and local optimization in Metropolis sampling. *Journal of the American Statistical Association*, 95(449):121–134, 2000.
- Roberto Casarin, Radu Craiu, and Fabrizio Leisen. Interacting multiple try algorithms with different proposal distribution. *Statistical Computing*, 23:185–200, 2013.
- Jinyoung Yang, Evgeny Levi, Radu Craiu, and Jeffrey S. Rosenthal. Adaptive component-wise multiple-try Metropolis sampling. *Journal of Computational and Graphical Statistics*, 28(2):276–289, 2019.
- Philippe Gagnon, Florian Maire, and Giacomo Zanella. Improving multiple-try Metropolis with local balancing. *Journal of Machine Learning Research*, 24:1–59, 2023.
- Silvia Pandolfi, Francesco Bartolucci, and Nial Friel. A generalization of the multiple-try Metropolis algorithm for Bayesian estimation and model selection. *Proceedings of the 13th international conference on artificial intelligence and statistics*, 2010.
- Silvia Pandolfi, Francesco Bartolucci, and Nial Friel. A generalized multiple-try version of the reversible jump algorithm. *Computational Statistics and Data Analysis*, 72:298–314, 2014.
- Simon Fontaine and Mylène Béard. An adaptive multiple-try Metropolis algorithm. *Bernoulli*, 28(3):1986–2011, 2022.
- Hugh Chipman and Derek Bingham. Let’s practice what we preach: Planning and interpreting simulation studies with design and analysis of experiments. *The Canadian Journal of Statistics*, 50(4):1228–1249, 2022.

- A. Gelman, C. Pasarica, and R. Dodhia. Let’s practice what we preach: Turning tables into graphs. *The American Statistician*, 56:121–130, 2002.
- M. Harwell, N. Kohli, and Y. Peralta. Experimental design and data analysis in computer simulation studies in the behavioral sciences. *Journal of Modern Applied Statistical Methods*, 16:3–28, 2017.
- A. Skrondal. Design and analysis of Monte Carlo experiments: Attacking the conventional wisdom. *Multivariate Behavioral Research*, 35:137–167, 2000.
- Luke Tierney. A note on Metropolis-Hastings kernels for general state spaces. *The Annals of Applied Probability*, 8(1): 1–9, 1998.
- Charles T. Geyer and Jesper Moller. Simulation procedures and likelihood inference for spatial point processes. *Scandinavian Journal of Statistics*, 21(4):359–373, 1994.
- Peter J. Green. Reversible jump Markov chain Monte Carlo computation and Bayesian model determination. *Biometrika*, 82(4):711–732, 1995.
- C. Andrieu and J. Thoms. A tutorial on adaptive MCMC. *Statistical Computing*, 18:343–373, 2008.
- G. O. Roberts, A. Gelman, and W. R. Gilks. Weak convergence and optimal scaling of random walk Metropolis algorithms. *Annals of Applied Probability*, 7(1):110–120, 1997.
- H. Haario, E. Saksman, and J. Tamminen. Adaptive proposal distribution for random walk Metropolis algorithm. *Computational Statistics*, 14:375–395, 1999.
- Jeff Bezanson, Alan Edelman, Stefan Karpinski, and Viral B Shah. Julia: A fresh approach to numerical computing. *SIAM review*, 59(1):65–98, 2017. URL <https://doi.org/10.1137/14100671>.
- R Core Team. *R: A Language and Environment for Statistical Computing*. R Foundation for Statistical Computing, Vienna, Austria, 2022. URL <https://www.R-project.org/>.
- Hadley Wickham. *ggplot2: Elegant Graphics for Data Analysis*. Springer-Verlag New York, 2016. ISBN 978-3-319-24277-4. URL <https://ggplot2.tidyverse.org>.
- Miguel Biron-Lattes, Nikola Surjanovic, Saifuddin Syed, Trevor Campbell, and Alexandre Bouchard-Côté. autoMALA: Locally adaptive Metropolis-adjusted Langevin algorithm, 2024. URL <https://arxiv.org/abs/2310.16782>.
- Dootika Vats, James M Flegal, and Galin L Jones. Multivariate output analysis for Markov chain Monte Carlo. *Biometrika*, 106:321–337, 2019. doi:<https://doi.org/10.1093/biomet/asz002>.
- Radford M. Neal. Slice sampling. *The Annals of Statistics*, 31(3):705–767, 2003.
- Chirag Modi, Alex Barnett, and Bob Carpenter. Delayed rejection Hamiltonian Monte Carlo for sampling multiscale distributions. *Bayesian Analysis*, 19(3):815–842, 2024.
- Stephen F Gull. *Maximum-entropy and Bayesian methods in Science and Engineering*, chapter Bayesian inductive inference and maximum entropy, pages 53–74. Springer, 1988.
- A. Gelman, J.B. Carlin, H.S. Stern, D.B. Dunson, A. Veharti, and D.B. Rubin. *Bayesian Data Analysis*. Chapman Hall/CRC, 3 edition, 2013.
- D.B. Rubin. Estimation in parallel randomized experiments. *Journal of Educational Statistics*, 6(4):377–401, 1981.

Supplementary Materials

Proof of Theorem 1

Before beginning the proof of Theorem 1, we present the following two lemmas. To simplify notation, we define $\tilde{\mathbf{x}}^* = g(\tilde{\mathbf{x}})$.

Lemma S1. *If Assumption 1 is satisfied, then the acceptance ratio*

$$r(\tilde{\mathbf{x}}^*) = \frac{\pi(g(\tilde{\mathbf{x}}^*))}{\tilde{\pi}(\tilde{\mathbf{x}}^*)} |J(g_C(\tilde{\mathbf{x}}_C^*))| \quad (10)$$

satisfies $r(\tilde{\mathbf{x}}^*) = 1/r(\tilde{\mathbf{x}})$.

Proof of Lemma S1. Since g is an involution, $g = g^{-1}$ and it follows that $|J(g(\tilde{\mathbf{x}}^*))| = |J(g^{-1}(\tilde{\mathbf{x}}^*))|$. From the inverse mapping theorem, $|J(g^{-1}(\tilde{\mathbf{x}}))| = |J(g(\tilde{\mathbf{x}}))^{-1}| = |J(g(\tilde{\mathbf{x}}))|^{-1}$. Therefore, $|J(g(\tilde{\mathbf{x}}^*))||J(g(\tilde{\mathbf{x}}))| = 1$. From this, we can show that

$$\begin{aligned} r(\tilde{\mathbf{x}}^*) &= \frac{\tilde{\pi}(g(\tilde{\mathbf{x}}^*))}{\tilde{\pi}(\tilde{\mathbf{x}}^*)} |J(g_C(\tilde{\mathbf{x}}^*))| \\ &= \frac{\tilde{\pi}(g(g(\tilde{\mathbf{x}})))}{\tilde{\pi}(g(\tilde{\mathbf{x}}))} |J(g_C(\tilde{\mathbf{x}}^*))| \\ &= \frac{\tilde{\pi}(\tilde{\mathbf{x}})}{\tilde{\pi}(g(\tilde{\mathbf{x}}))} \frac{1}{|J(g_C(\tilde{\mathbf{x}}))|} \\ &= \frac{1}{r(\tilde{\mathbf{x}})}. \end{aligned}$$

□

Proof of Theorem 1. Suppose we have a random vector $\tilde{\mathbf{x}} \sim \tilde{\pi}$, the current state, and a vector $\tilde{\mathbf{y}}$ as the state after completing an iteration of the algorithm. For two sets A and B , the proof will be completed by showing that the statement of detailed balance [Green, 1995] below holds true,

$$P(\tilde{\mathbf{x}} \in A, \tilde{\mathbf{y}} \in B) = P(\tilde{\mathbf{x}} \in B, \tilde{\mathbf{y}} \in A). \quad (11)$$

Consider two cases of the value of $\tilde{\mathbf{y}}$: the proposal is rejected and $\tilde{\mathbf{x}} = \tilde{\mathbf{y}}$, and the proposal is accepted and $\tilde{\mathbf{y}} = g(\tilde{\mathbf{x}}) \neq \tilde{\mathbf{x}}$. Since these are disjoint events, the LHS of Equation 11 can be written as

$$P(\tilde{\mathbf{x}} \in A, \tilde{\mathbf{y}} \in B) = P(\tilde{\mathbf{x}} \in A, \tilde{\mathbf{y}} \in B, \tilde{\mathbf{x}} = \tilde{\mathbf{y}}) + P(\tilde{\mathbf{x}} \in A, \tilde{\mathbf{y}} \in B, \tilde{\mathbf{x}} \neq \tilde{\mathbf{y}}).$$

Therefore, to show that Equation 11 holds, it is sufficient to show that the two terms of the RHS above are symmetric. The first term is trivially symmetric about $\tilde{\mathbf{x}}$ and $\tilde{\mathbf{y}}$. For the second term, consider the the additional sets $\tilde{B} = \{g(\mathbf{x}) : \mathbf{x} \in A, g(\mathbf{x}) \neq \mathbf{x}\}$, the image of g , and $\tilde{A} = g^{-1}(\tilde{B})$, the pre-image of \tilde{B} w.r.t. g . Since $\tilde{\mathbf{y}}$ is defined as a deterministic transformation of $\tilde{\mathbf{x}}$, all events outside these domains occur with probability zero and the second term can be further simplified as

$$P(\tilde{\mathbf{x}} \in A, \tilde{\mathbf{y}} \in B, \tilde{\mathbf{x}} \neq \tilde{\mathbf{y}}) = P(\tilde{\mathbf{x}} \in \tilde{A}, \tilde{\mathbf{y}} \in \tilde{B}, \tilde{\mathbf{x}} \neq \tilde{\mathbf{y}}),$$

which we want to show satisfies symmetry

$$P(\tilde{\mathbf{x}} \in \tilde{A}, \tilde{\mathbf{y}} \in \tilde{B}, \tilde{\mathbf{x}} \neq \tilde{\mathbf{y}}) = P(\tilde{\mathbf{x}} \in \tilde{B}, \tilde{\mathbf{y}} \in \tilde{A}, \tilde{\mathbf{x}} \neq \tilde{\mathbf{y}}). \quad (12)$$

Evaluating Equation 12 gives:

$$\sum_{\tilde{\mathbf{x}}_D \in \tilde{A}_D} \int_{\tilde{\mathbf{x}}_C \in \tilde{A}_C} \tilde{\pi}(\tilde{\mathbf{x}}) a(\tilde{\mathbf{x}}) d\tilde{\mathbf{x}}_C = \sum_{\tilde{\mathbf{x}}_D \in \tilde{A}_D} \int_{\tilde{\mathbf{x}}_C \in \tilde{A}_C} \tilde{\pi}(g(\tilde{\mathbf{x}})) a(g(\tilde{\mathbf{x}})) |J(g(\tilde{\mathbf{x}}_C))| d\tilde{\mathbf{x}}_C,$$

where $a(\tilde{\mathbf{x}}) = 1 \wedge r(\tilde{\mathbf{x}})$ and $r(\tilde{\mathbf{x}})$ is defined in Equation 10. This equality is satisfied if

$$\tilde{\pi}(\tilde{\mathbf{x}}) a(\tilde{\mathbf{x}}) = \tilde{\pi}(g(\tilde{\mathbf{x}})) a(g(\tilde{\mathbf{x}})) |J(g_C(\tilde{\mathbf{x}}_C))|.$$

The above detailed balance criteria can be rewritten as:

$$\tilde{\pi}(\tilde{\mathbf{x}}) a(\tilde{\mathbf{x}}) = \tilde{\pi}(\tilde{\mathbf{x}}^*) a(\tilde{\mathbf{x}}^*) |J(g_C(\tilde{\mathbf{x}}_C))|. \quad (13)$$

To show that Equation 13 holds, we consider two cases separately: $a(\tilde{\mathbf{x}}) = 1$ and $a(\tilde{\mathbf{x}}) < 1$. In the first case, we know that $r(\tilde{\mathbf{x}}) \geq 1$, so by Lemma S1 $r(\tilde{\mathbf{x}}^*) \leq 1$. In particular,

$$r(\tilde{\mathbf{x}}^*) = \frac{\tilde{\pi}(g(\tilde{\mathbf{x}}^*))}{\tilde{\pi}(\tilde{\mathbf{x}}^*)} |J(g_C(\tilde{\mathbf{x}}^*))| = \frac{\tilde{\pi}(\tilde{\mathbf{x}})}{\tilde{\pi}(g(\tilde{\mathbf{x}}))} \frac{1}{|J(g_C(\tilde{\mathbf{x}}))|}.$$

Substituting this back into Equation 13 and simplifying to show that the right-hand and left-hand sides of the equation are equal yields

$$\begin{aligned} \tilde{\pi}(\tilde{\mathbf{x}}) a(\tilde{\mathbf{x}}) &= \tilde{\pi}(\tilde{\mathbf{x}}^*) a(\tilde{\mathbf{x}}^*) |J(g_C(\tilde{\mathbf{x}}_C))| \\ \tilde{\pi}(\tilde{\mathbf{x}}) &= \tilde{\pi}(\tilde{\mathbf{x}}^*) \frac{\tilde{\pi}(\tilde{\mathbf{x}})}{\tilde{\pi}(\tilde{\mathbf{x}}^*)} \frac{|J(g_C(\tilde{\mathbf{x}}_C))|}{|J(g_C(\tilde{\mathbf{x}}_C))|} \\ \tilde{\pi}(\tilde{\mathbf{x}}) &= \tilde{\pi}(\tilde{\mathbf{x}}). \end{aligned}$$

The second case is $a(\tilde{\mathbf{x}}) < 1 = r(\tilde{\mathbf{x}})$, which implies that $r(\tilde{\mathbf{x}}^*) > 1$ and so $a(\tilde{\mathbf{x}}^*) = 1$. Plugging these into Equation 13 give us

$$\begin{aligned}\tilde{\pi}(\tilde{\mathbf{x}})a(\tilde{\mathbf{x}}) &= \tilde{\pi}(\tilde{\mathbf{x}}^*)a(\tilde{\mathbf{x}}^*)|J(g_C(\tilde{\mathbf{x}}_C))| \\ \tilde{\pi}(\tilde{\mathbf{x}})\frac{\tilde{\pi}(\tilde{\mathbf{x}}^*)}{\tilde{\pi}(\tilde{\mathbf{x}})}|J(g_C(\tilde{\mathbf{x}}_C))| &= \tilde{\pi}(\tilde{\mathbf{x}}^*)|J(g_C(\tilde{\mathbf{x}}_C))| \\ \tilde{\pi}(\tilde{\mathbf{x}}^*)|J(g_C(\tilde{\mathbf{x}}_C))| &= \tilde{\pi}(\tilde{\mathbf{x}}^*)|J(g_C(\tilde{\mathbf{x}}_C))|.\end{aligned}$$

Since Equation 13 is satisfied in both cases, this is sufficient to show that detailed balance is preserved through the procedure outlined in Section 2.1. This concludes the proof of the validity of the procedure. \square

Pseudocode

In this section of the Supplementary Materials we include the pseudocode for the ad hoc procedure used to automatically determine the burn-in period for each sample.

Algorithm 5 Automatic burn-in

- 1: **Input:** Monte Carlo sample $\{\mathbf{x}_n\}_{n=1}^N$.
 - 2: Split chain into 20 equally-sized blocks: $n_j = j \times \lfloor N/20 \rfloor$, $j = 0, \dots, 20$.
 - 3: Initialize sample to final block: $\mathcal{X} = \{\mathbf{x}_n\}_{n_{19}}^N$, $N_0 = n_{19}$.
 - 4: Compute $(L(\mathcal{X}), U(\mathcal{X}))$ as the empiric 95% interval of \mathcal{X} .
 - 5: **for** $j \in \{18, \dots, 1\}$ **do**
 - 6: Compute mean of next block $\mu = \frac{1}{\lfloor N/20 \rfloor} \sum_{i=n_{j-1}}^{n_j} \mathbf{x}_i$.
 - 7: **if** $\mu \in (L(\mathcal{X}), U(\mathcal{X}))$ **then**
 - 8: Update our sample: $\mathcal{X} = \{\mathbf{x}_n\}_{n_{j-1}}^N$.
 - 9: Update the 95% interval: $(L(\mathcal{X}), U(\mathcal{X}))$.
 - 10: Update the burn-in index: $N_0 = n_{j-1}$.
 - 11: **end if**
 - 12: **if** $\mu \notin (L(\mathcal{X}), U(\mathcal{X}))$ for 2 consecutive samples **then**
 - 13: Return burn-in N_0 and sample \mathcal{X} .
 - 14: **end if**
 - 15: **end for**
-

Additional Figures

In this section of the Supplementary Materials we include additional results from the simulation study conducted in Section 4.

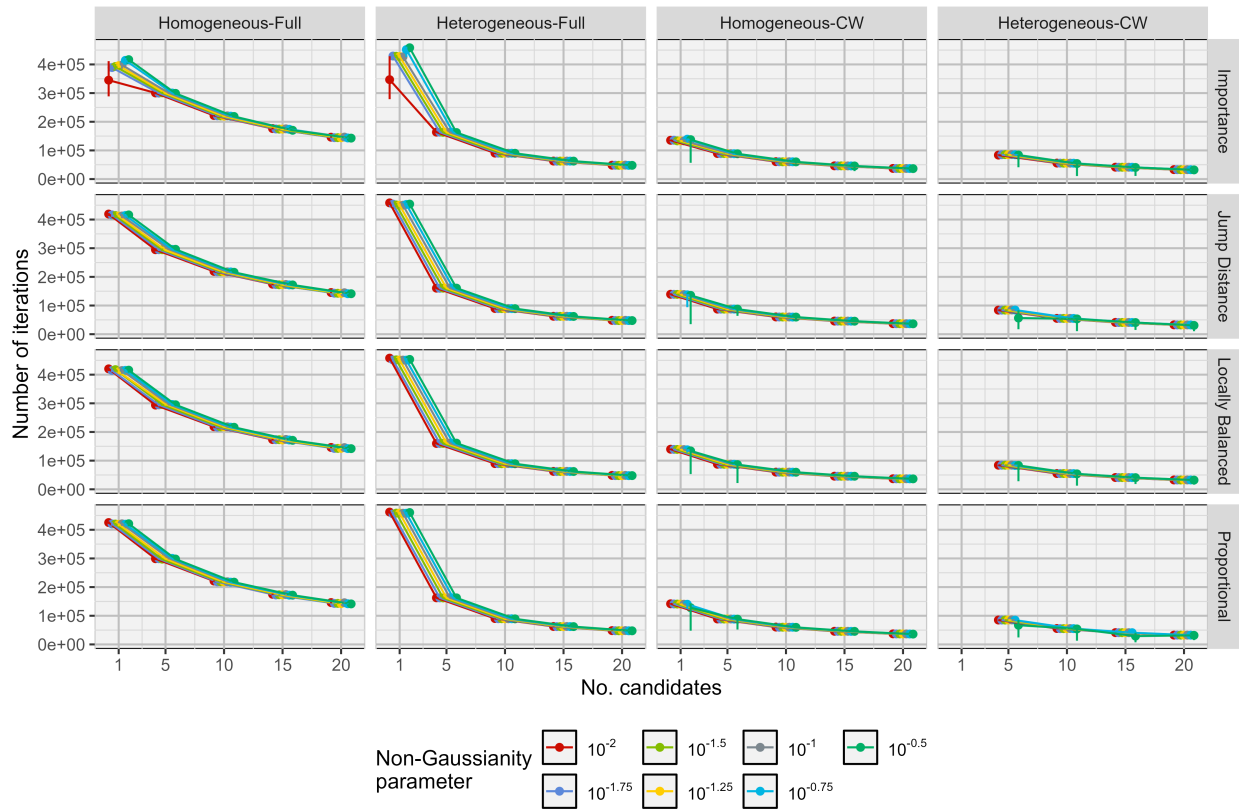


Figure 11: Number of iterations produced by each algorithm in 15 seconds, both before and after removing burn-in samples. Results for the weight function are aggregated as the evaluation time for all weight functions should be similar in this case. Panels correspond to the proposal distribution.

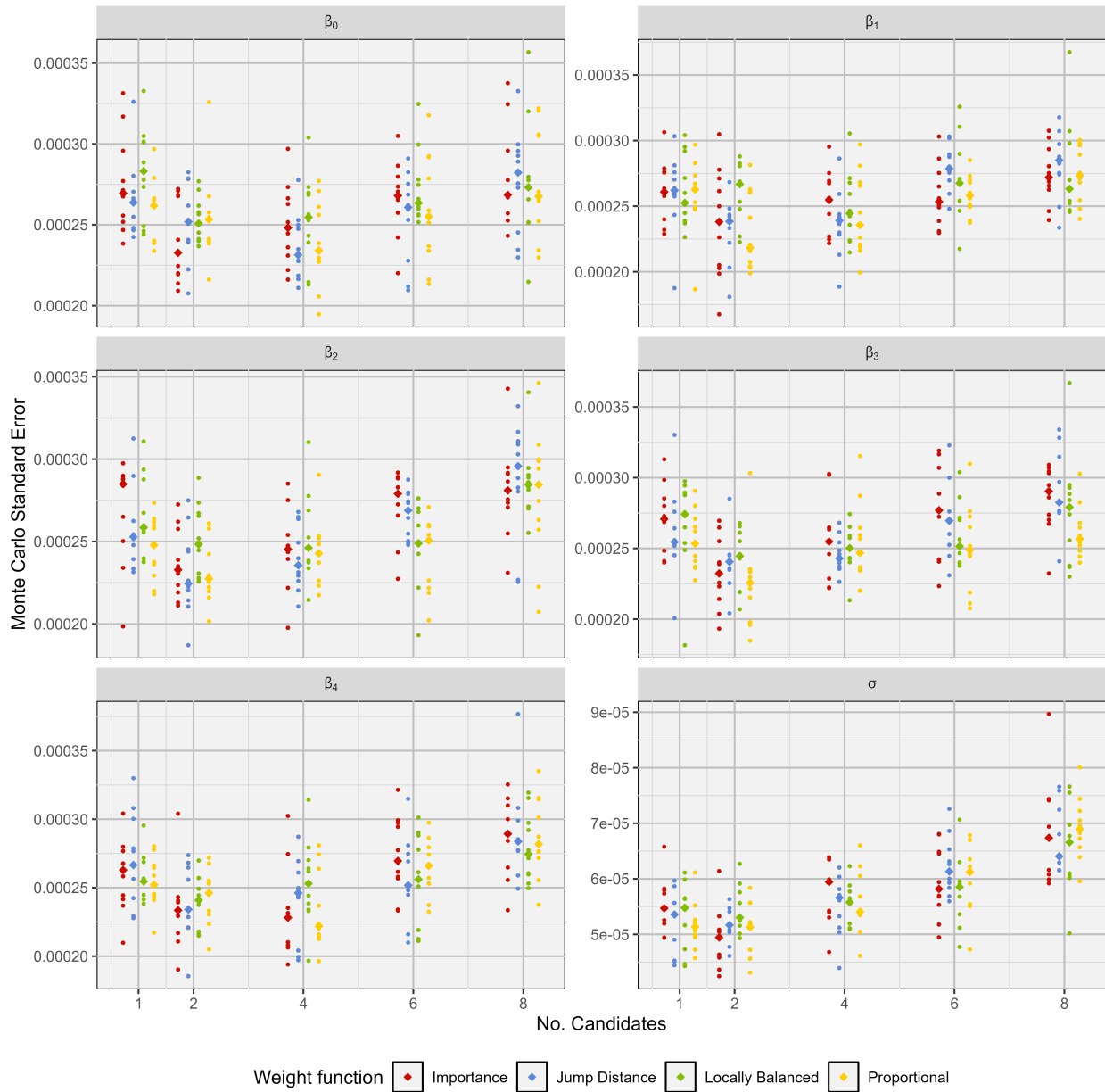


Figure 12: Monte Carlo standard errors for the Homogeneous-Full proposal distribution. Small points are the MCSE for each data seed and large points are the median MCSE over all seeds. Results for $M = 10$ are omitted.

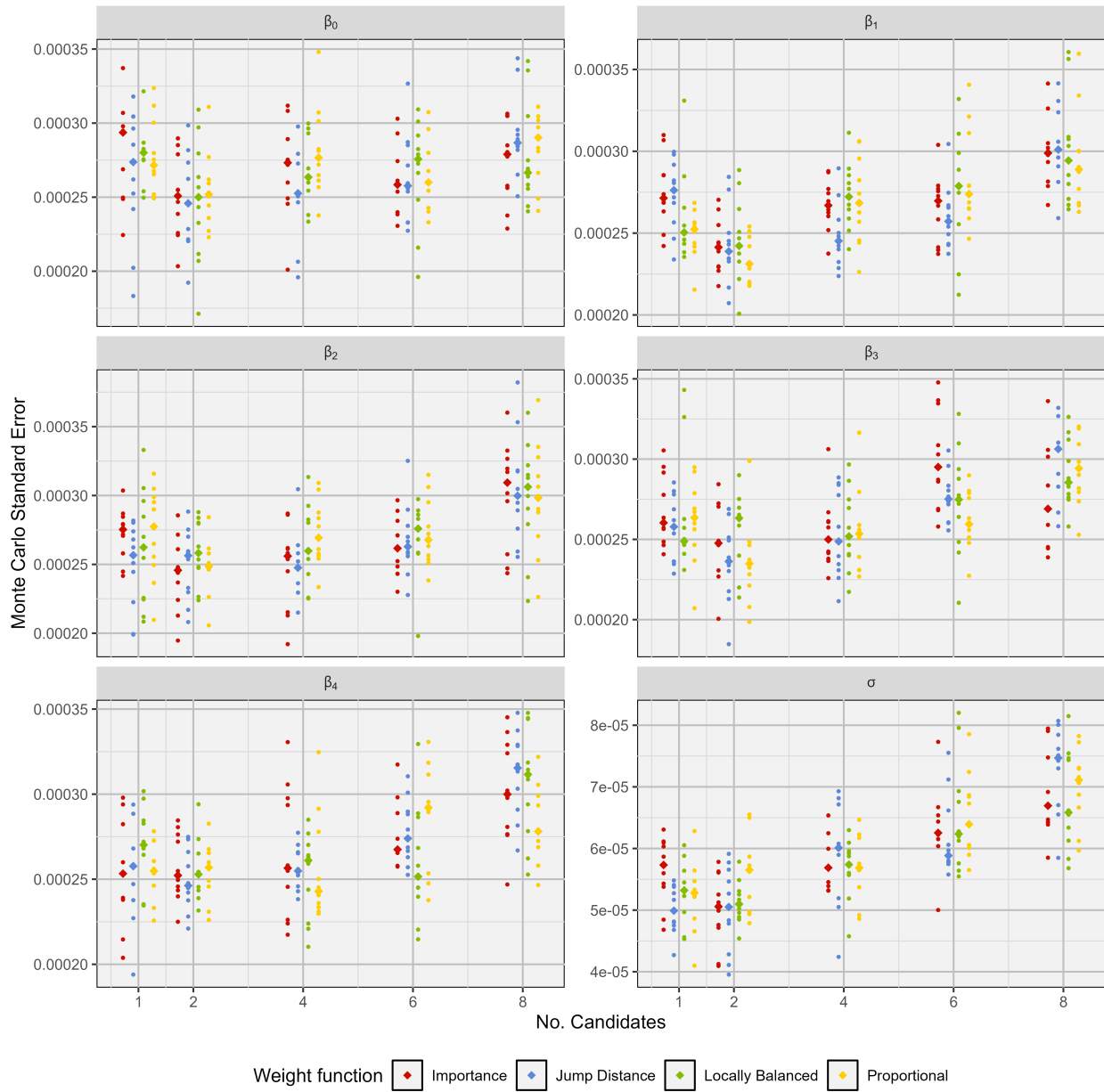


Figure 13: Monte Carlo standard errors for the Heterogeneous-Full proposal distribution. Small points are the MCSE for each data seed and large points are the median MCSE over all seeds. Results for $M = 10$ are omitted.

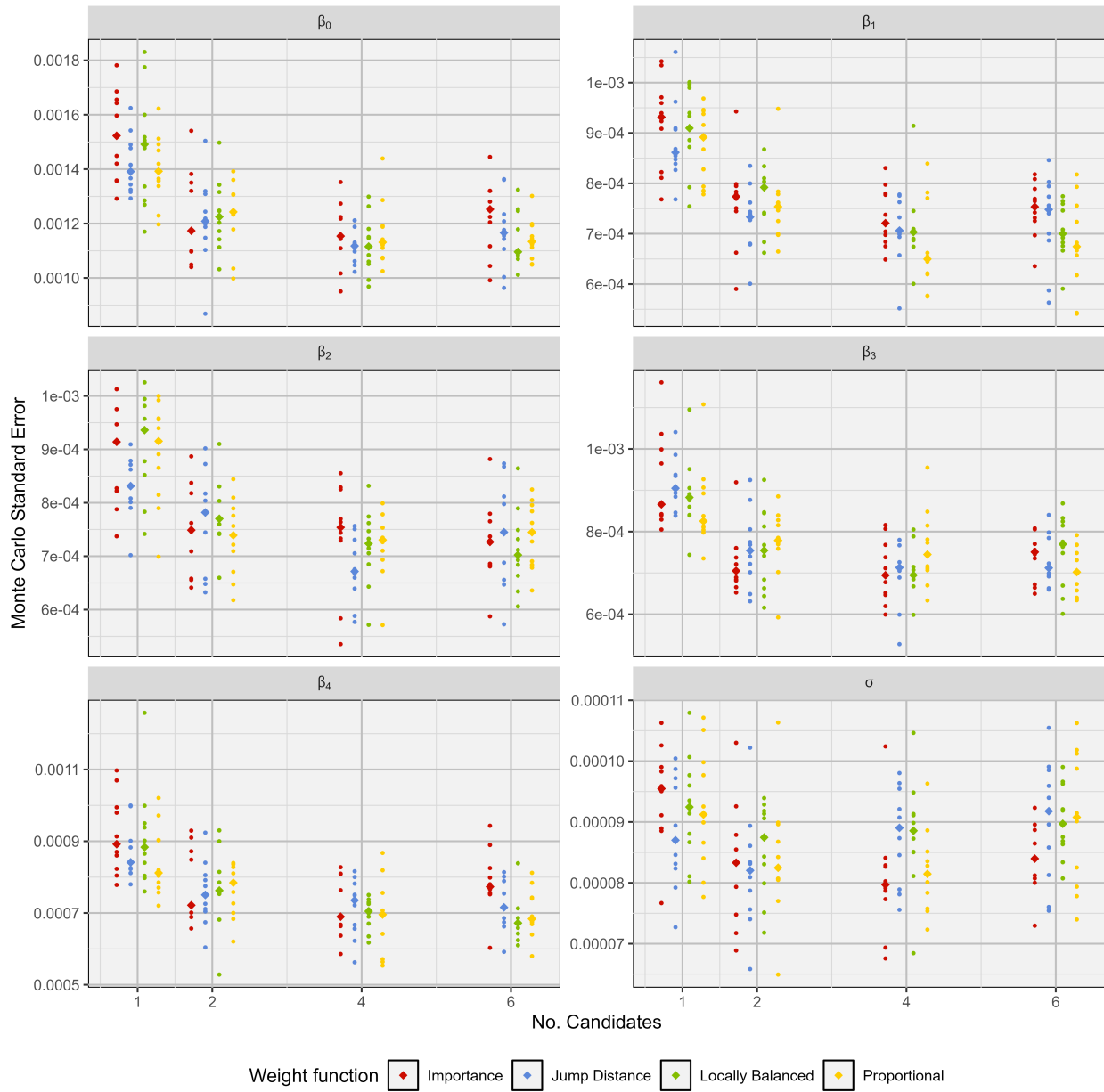


Figure 14: Monte Carlo standard errors for the Homogeneous-CW proposal distribution. Small points are the MCSE for each data seed and large points are the median MCSE over all seeds. Results for $M = 8, 10$ are omitted.

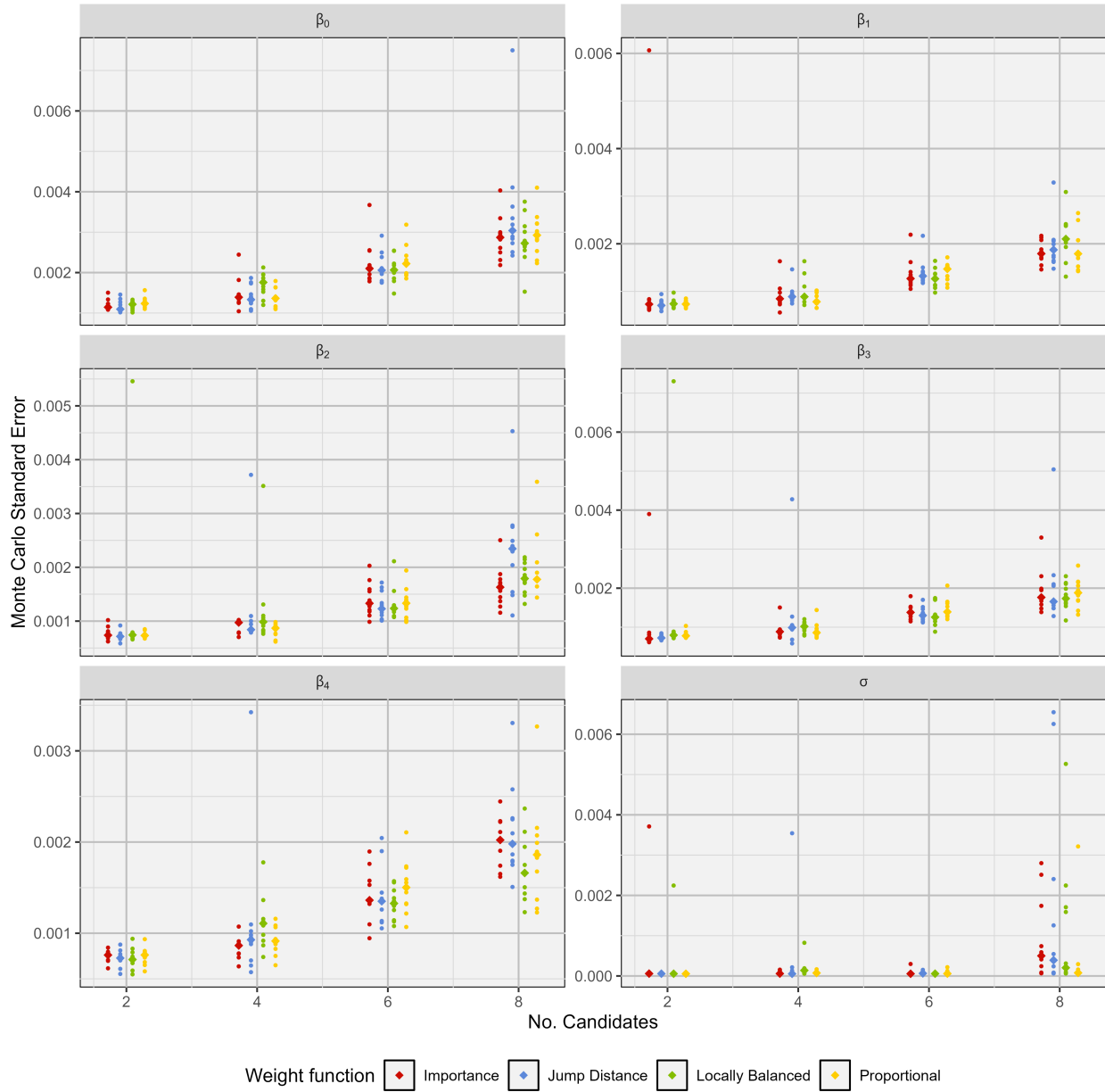


Figure 15: Monte Carlo standard errors for the Heterogeneous-CW proposal distribution. Small points are the MCSE for each data seed and large points are the median MCSE over all seeds. Results for $M = 10$ are omitted.